



Review

Aspergillus nidulans—Natural Metabolites Powerhouse: Structures, Biosynthesis, Bioactivities, and Biotechnological Potential

Kholoud F. Ghazawi ¹, Sarah A. Fatani ², Shaimaa G. A. Mohamed ³, Gamal A. Mohamed ⁴ 
and Sabrin R. M. Ibrahim ^{5,6,*} 

¹ Clinical Pharmacy Department, College of Pharmacy, Umm Al-Qura University, Makkah 24382, Saudi Arabia; kfgghazawi@uqu.edu.sa

² Department of Clinical Pharmacy, Prince Sattam Bin Abdulaziz University, Al-Kharj 11942, Saudi Arabia

³ Faculty of Dentistry, British University, El Sherouk City, Suez Desert Road, Cairo 11837, Egypt; shaimaag1973@gmail.com

⁴ Department of Natural Products and Alternative Medicine, Faculty of Pharmacy, King Abdulaziz University, Jeddah 21589, Saudi Arabia

⁵ Preparatory Year Program, Department of Chemistry, Batterjee Medical College, Jeddah 21442, Saudi Arabia

⁶ Department of Pharmacognosy, Faculty of Pharmacy, Assiut University, Assiut 71526, Egypt

* Correspondence: sabrin.ibrahim@bmc.edu.sa or sabreen.ibrahim@pharm.aun.edu.eg; Tel.: +966-581-1830-34

Abstract: Nowadays, finding out new natural scaffolds of microbial origin increases at a higher rate than in the past decades and represents an auspicious route for reinvigorating the pool of compounds entering pharmaceutical industries. Fungi serve as a depository of fascinating, structurally unique metabolites with considerable therapeutic significance. *Aspergillus* genus represents one of the most prolific genera of filamentous fungi. *Aspergillus nidulans* Winter G. is a well-known and plentiful source of bioactive metabolites with abundant structural diversity, including terpenoids, benzophenones, sterols, alkaloids, xanthenes, and polyketides, many of which display various bioactivities, such as cytotoxicity, antioxidant, anti-inflammatory, antiviral, and antimicrobial activities. The current work is targeted to survey the reported literature on *A. nidulans*, particularly its metabolites, biosynthesis, and bioactivities, in addition to recent reports on its biotechnological potential. From 1953 till November 2022, relying on the stated data, 206 metabolites were listed, with more than 100 references.

Keywords: fungi; *Aspergillus nidulans*; *Trichocomaceae*; metabolites; biosynthesis; biotechnological potential; life on land; drug discovery



Citation: Ghazawi, K.F.; Fatani, S.A.; Mohamed, S.G.A.; Mohamed, G.A.; Ibrahim, S.R.M. *Aspergillus nidulans*—Natural Metabolites Powerhouse: Structures, Biosynthesis, Bioactivities, and Biotechnological Potential. *Fermentation* **2023**, *9*, 325. <https://doi.org/10.3390/fermentation9040325>

Academic Editors: Xiaofei Tian and Mónica Gandía

Received: 23 February 2023

Revised: 13 March 2023

Accepted: 23 March 2023

Published: 25 March 2023



Copyright: © 2023 by the authors. Licensee MDPI, Basel, Switzerland. This article is an open access article distributed under the terms and conditions of the Creative Commons Attribution (CC BY) license (<https://creativecommons.org/licenses/by/4.0/>).

1. Introduction

With the increase in the burden of non-communicable diseases, as well as the growing antimicrobial-resistant infections, the need for new agents that can supply amended therapeutic outcomes has taken on the utmost primacy. Therefore, the investigation of microbes is one of the auspicious ways of finding out lead molecules for drug discovery. Fungi are among the microbes that possess enormous negative and positive influences on human lives [1,2]. They serve as a depository of biometabolites that represent the backbone of different available pharmaceuticals. Moreover, fascinating, structurally unique metabolites, with considerable therapeutic significance as antibiotics as well as anticancer, antidiabetic, antiviral, and immuno-suppressive agents, have been reported in these untapped microorganisms [3–13]. In addition, they have proved to be superbly efficient decomposers and have developed the capacity to feed on and break down polymeric substances and organic matter by secreting various enzymes, providing sustainable solutions for diverse industries and markets [7,14,15].

Additionally, fungal biotechnology may assist human society's transition from a petroleum-dependent to a bio-based circular economy. Moreover, they are able to sustainably produce feed, food, chemicals, textiles, fuels, and more [1,2]. On the other hand,

they also manufacture toxins that spoil different foods, and they predominantly infect immuno-compromised patients, which drives up public health costs [1,2].

The *Aspergillus* genus (*Trichocomaceae*, class *Discellaceae*), with more than 400 species, represents one of the most prolific genera of filamentous fungi [16]. *Aspergillus* is an anamorphic (asexual) genus; some of its species have teleomorphs (sexual states), such as *A. nidulans*, which in its sexual state is called *Emericella nidulans* [17]. Its species are encountered in outdoor and indoor environments and have relevant medical, food, and industrial applications [16–19]. Additionally, this genus is renowned for its biosynthesizing of diverse classes of metabolites with myriad bioactivities [5,16,20,21]. Moreover, some of its species have potential biotechnological and industrial applications [16,22]. On the other hand, some cause diverse illnesses to animals and humans [23,24].

Among this species, *Aspergillus nidulans* Winter G was reported to cause cerebral aspergillosis and is a common pathogen in patients with chronic granulomatous disease [25–27]. *A. nidulans* is well known for its plentiful sources of bioactive metabolites with abundant structural diversity, including terpenoids, alkaloids, polyketides, many of which display various biological activities, such as antioxidant, antialgal, anti-mycobacterial, antiviral, plant growth promoting, cytotoxicity, anti-inflammatory, and antimicrobial activities. In addition, *A. nidulans* has the potential to secrete various enzymes: laccase, β -glucosidase, keratinase, cellulase, xylanase, lipase, β -galactosidase, cutinase, protease, tannase, and aryl alcohol oxidase [28]. It is noteworthy that the *A. nidulans* genetic model has been extensively studied regarding cellular development, metabolism, and gene regulation, contributing to an understanding of eukaryotic cell biology and molecular processes, where the capabilities of its genetic manipulation and combining of genetic traits via sexual crossing are important for its marked function as a genetic model [29].

The prime aim of this work is to focus on the stated research on *A. nidulans* collected from various sources, particularly the structures, biosynthesis, and bioactivities of its metabolites. Moreover, recent reports on its biotechnological relevance, as well as nanoparticle synthesis, have been reviewed. Reported studies from 1953 to November 2022 are presented. The molecular formulae and weights, chemical classes, hosts, location, and bioactivities for its metabolites are listed. The structures of these metabolites according to their chemical classes are summarized. The present work could provide a guide for future expected research exploring the untapped potential of *A. nidulans* as one of the prosperous producers of bio-metabolites.

2. Methodology

2.1. Data Collection

A survey of the literature was done using assorted databases and publishers: Scopus, PubMed, GoogleScholar, ScienceDirect, Wiley, Taylor & Francis, Bentham, Thieme, MDPI, and Springer. The search was carried out using “*Aspergillus nidulans* + compounds”, OR “*Aspergillus nidulans* + NMR”, OR “*Aspergillus nidulans* + biosynthesis”, OR “*Aspergillus nidulans* + Biological activity”, “*Aspergillus nidulans* + Biotechnology”, “*Aspergillus nidulans* + Enzymes”, OR “*Aspergillus nidulans* + nanoparticles” as keywords. All chemical structures were drawn utilizing ChemDraw.

2.2. Data Selection

The criteria for the reported data selection included in this review were: (1) studies that reported *A. nidulans*’ metabolites, including their structures, biosynthesis, and bioactivities, as well as biotechnological importance and nanoparticle synthesis using *A. nidulans*; (2) all the reported data published in peer-reviewed journals (e.g., articles, reviews, abstracts); and (3) reviews and book chapters. Included studies were assessed through reading of titles, abstracts, and full texts. For non-English articles, the data were extracted from the English abstracts. In this work, published data covering the period from 1953 to November 2022 have been included. In the current work, 103 references have been cited, including various articles and books.

3. Metabolites of *Aspergillus nidulans* and their Bioactivities

Several studies reported the separation and characterization of assorted classes of metabolites, employing various chromatographic and spectral tools that are surveyed herein, along with their estimated bioactivities and postulated biosynthesis pathways. It was noted that among the diverse metabolites reported from this species, a limited number of them have been assessed for biological capacity (Table 1).

Table 1. Biological activity of reported metabolites from *Aspergillus nidulans*.

Compound Name	Biological Activity	Assay, Organism or Cell Line	Biological Compound	Results Positive Control	Ref.
Isosecosterigmatocystin (15)	Antimicrobial	Microplate/ <i>Edwardsiella ictaluri</i>	16.0 µg/mL (MIC)	Chloramphenicol 0.5 µg/mL (MIC)	[30]
		Serial dilution/ <i>Edwardsiella ictarda</i>	16.0 µg/mL (MIC)	Chloramphenicol 2.0 µg/mL (MIC)	[31]
Sterigmatocystin (18)	Antimicrobial	Serial dilution/ <i>Vibrio parahaemolyticus</i>	64.0 µg/mL (MIC)	Chloramphenicol 0.5 µg/mL (MIC)	[31]
Versicolorin C (35)	Antimicrobial	Microplate/ <i>Escherichia coli</i>	1.0 µg/mL (MIC)	Chloramphenicol 1.0 µg/mL (MIC)	[30]
		Microplate/ <i>Micrococcus luteus</i>	32.0 µg/mL (MIC)	Chloramphenicol 2.0 µg/mL (MIC)	[30]
		Microplate/ <i>Vibrio anguillarum</i>	4.0 µg/mL (MIC)	Chloramphenicol 1.0 µg/mL (MIC)	[30]
		Microplate/ <i>Vibrio alginolyticus</i>	16.0 µg/mL (MIC)	Chloramphenicol 0.5 µg/mL (MIC)	[30]
		Microplate/ <i>Edwardsiella ictaluri</i>	8.0 µg/mL (MIC)	Chloramphenicol 0.5 µg/mL (MIC)	[30]
		Microplate/ <i>Vibrio parahaemolyticus</i>	1.0 µg/mL (MIC)	Chloramphenicol 2.0 µg/mL (MIC)	[30]
Isoversicolorin C (36)	Antimicrobial	Microplate/ <i>Escherichia coli</i>	32.0 µg/mL (MIC)	Chloramphenicol 1.0 µg/mL (MIC)	[30]
		Microplate/ <i>Micrococcus luteus</i>	16.0 µg/mL (MIC)	Chloramphenicol 2.0 µg/mL (MIC)	[30]
		Microplate/ <i>Vibrio vulnificus</i>	64.0 µg/mL (MIC)	Chloramphenicol 8.0 µg/mL (MIC)	[30]
		Microplate/ <i>Vibrio alginolyticus</i>	1.0 µg/mL (MIC)	Chloramphenicol 0.5 µg/mL (MIC)	[30]
		Microplate/ <i>Edwardsiella ictaluri</i>	4.0 µg/mL (MIC)	Chloramphenicol 0.5 µg/mL (MIC)	[30]
		Microplate/ <i>Vibrio parahaemolyticus</i>	32.0 µg/mL (MIC)	Chloramphenicol 2.0 µg/mL (MIC)	[30]
Violaceol I (52)	Antimicrobial	Microdilution/ <i>Bacillus subtilis</i>	13.0 µg/mL (MIC)	Chloramphenicol 6.3 µg/mL (MIC)	[32]
Violaceol II (53)	Antimicrobial	Microdilution/ <i>Bacillus subtilis</i>	50 µg/mL (MIC)	Chloramphenicol 6.3 µg/mL (MIC)	[32]
Diorcinol (54)	Antimicrobial	Microdilution/ <i>Bacillus subtilis</i>	100.0 µg/mL (MIC)	Chloramphenicol 6.3 µg/mL (MIC)	[32]
Cordylol C (55)	Antimicrobial	Microdilution/ <i>Bacillus subtilis</i>	100.0 µg/mL (MIC)	Chloramphenicol 6.3 µg/mL (MIC)	[32]
Gibellulin A (56)	Antimicrobial	Serial dilution/ <i>Aeromonas hydrophila</i>	4.0 µg/mL (MIC)	Chloramphenicol 0.5 µg/mL (MIC)	[31]
		Serial dilution/ <i>Colletotrichum gloeosporioides</i>	4.0 µg/mL (MIC)	Amphotericin B 0.5 µg/mL (MIC)	[31]
		Serial dilution/ <i>Edwardsiella ictarda</i>	2.0 µg/mL (MIC)	Chloramphenicol 2.0 µg/mL (MIC)	[31]
		Serial dilution/ <i>Edwardsiella tarda</i>	4.0 µg/mL (MIC)	Chloramphenicol 0.5 µg/mL (MIC)	[31]
		Serial dilution/ <i>Escherichia coli</i>	8.0 µg/mL (MIC)	Chloramphenicol 1.0 µg/mL (MIC)	[31]
		Serial dilution/ <i>Vibrio alginolyticus</i>	8.0 µg/mL (MIC)	Chloramphenicol 0.5 µg/mL (MIC)	[31]
		Serial dilution/ <i>Vibrio harvey</i>	4.0 µg/mL (MIC)	Chloramphenicol 1.0 µg/mL (MIC)	[31]
		Serial dilution/ <i>Vibrio parahaemolyticus</i>	16.0 µg/mL (MIC)	Chloramphenicol 0.5 µg/mL (MIC)	[31]

Table 1. Cont.

Compound Name	Biological Activity	Assay, Organism or Cell Line	Biological Results		Ref.
			Compound	Positive Control	
Aspoquinolone E (65)	Cytotoxicity	MTT/HL-60	29.15 µM (IC ₅₀)	<i>cis</i> -platin 3.22 µM (IC ₅₀)	[33]
		MTT/A-549	3.50 µM (IC ₅₀)	<i>cis</i> -platin 13.17 µM (IC ₅₀)	[33]
		MTT/MCF-7	24.50 µM (IC ₅₀)	<i>cis</i> -platin 22.96 µM (IC ₅₀)	[33]
Aniduquinolone B (68)	Cytotoxicity	Brine shrimp lethality / <i>Artemia salina</i>	7.1 µM (LD ₅₀)	Colchicine 88.4 µM (LD ₅₀)	[34]
6-Deoxyaflaquinolone E (70)	Cytotoxicity	Brine shrimp lethality / <i>Artemia salina</i>	4.5 µM (LD ₅₀)	Colchicine 88.4 µM (LD ₅₀)	[34]
Aflaquinolone A (73)	Cytotoxicity	Brine shrimp lethality / <i>Artemia salina</i>	5.5 µM (LD ₅₀)	Colchicine 88.4 µM (LD ₅₀)	[34]
Aniquinazoline A (74)	Cytotoxicity	Brine shrimp lethality / <i>Artemia salina</i>	1.27 µM (LD ₅₀)	Colchicine 88.4 µM (LD ₅₀)	[35]
Aniquinazoline B (75)	Cytotoxicity	Brine shrimp lethality / <i>Artemia salina</i>	2.11 µM (LD ₅₀)	Colchicine 88.4 µM (LD ₅₀)	[35]
Aniquinazoline C (76)	Cytotoxicity	Brine shrimp lethality / <i>Artemia salina</i>	4.95 µM (LD ₅₀)	Colchicine 88.4 µM (LD ₅₀)	[35]
Aniquinazoline D (77)	Cytotoxicity	Brine shrimp lethality / <i>Artemia salina</i>	3.42 µM (LD ₅₀)	Colchicine 88.4 µM (LD ₅₀)	[35]
Glulisine A (81)	Antimicrobial	Microplate / <i>Edwardsiella ictaluri</i>	64.0 µg/mL (MIC)	Chloramphenicol 0.5 µg/mL (MIC)	[30]
Emestrin (82)		MTT/T47D	1.8 µg/mL (IC ₅₀)	-	[36]
		MTT/HepG2	4.2 µg/mL (IC ₅₀)	-	
		MTT/C28	2.6 µg/mL (IC ₅₀)	-	
		MTT/HeLa	13.8 µg/mL (IC ₅₀)	-	
Emestrin B (83)		MTT/T47D	0.16 µg/mL (IC ₅₀)	-	[37]
		MTT/HeLa	1.56 µg/mL (IC ₅₀)	-	
		MTT/WiDr	and 1.02 µg/mL (IC ₅₀)	-	
3,3'-Diindolylmethane (91)	Antimicrobial	Serial dilution / <i>Aeromonas hydrophilia</i>	64.0 µg/mL (MIC)	Chloramphenicol 0.5 µg/mL (MIC)	[31]
		Serial dilution / <i>Colletotrichum gloeosporioides</i>	64.0 µg/mL (MIC)	Amphotericin B 0.5 µg/mL (MIC)	[31]
		Serial dilution / <i>Edwardsiella tarda</i>	64.0 µg/mL (MIC)	Chloramphenicol 0.5 µg/mL (MIC)	[31]
Terrequinone A (92)	Antimicrobial	Serial dilution / <i>Aeromonas hydrophilia</i>	64.0 µg/mL (MIC)	Chloramphenicol 0.5 µg/mL (MIC)	[31]
		Serial dilution / <i>Colletotrichum gloeosporioides</i>	2.0 µg/mL (MIC)	Amphotericin B 0.5 µg/mL (MIC)	[31]
		Serial dilution / <i>Edwardsiella tarda</i>	16.0 µg/mL (MIC)	Chloramphenicol 0.5 µg/mL (MIC)	[31]
		Serial dilution / <i>Escherichia coli</i>	2.0 µg/mL (MIC)	Chloramphenicol 1.0 µg/mL (MIC)	[31]
		Serial dilution / <i>Vibrio alginolyticus</i>	2.0 µg/mL (MIC)	Chloramphenicol 0.5 µg/mL (MIC)	[31]
		Serial dilution / <i>Vibrio harvey</i>	64.0 µg/mL (MIC)	Chloramphenicol 1.0 µg/mL (MIC)	[31]
		Serial dilution / <i>Vibrio parahaemolyticus</i>	32.0 µg/mL (MIC)	Chloramphenicol 0.5 µg/mL (MIC)	[31]
19-Hydroxypenitrem A (93)	Cytotoxicity	Brine shrimp lethality / <i>Artemia salina</i>	3.2 µM (LD ₅₀)	Colchicine 10.7 µM (LD ₅₀)	[38]
	Antibacterial	Well diffusion / <i>Escherichia coli</i>	16.0 µg/mL (MIC)	Chloramphenicol 2.0 µg/mL (MIC)	[38]
		Well diffusion / <i>Edwardsiella tarda</i>	16.0 µg/mL (MIC)	Chloramphenicol 16.0 µg/mL (MIC)	[38]
		Well diffusion / <i>S. aureus</i>	16.0 µg/mL (MIC)	Chloramphenicol 2.0 µg/mL (MIC)	[38]
		Well diffusion / <i>Vibrio anguillarum</i>	32.0 µg/mL (MIC)	Chloramphenicol 0.5 µg/mL (MIC)	[38]

Table 1. Cont.

Compound Name	Biological Activity	Assay, Organism or Cell Line	Biological Results Compound	Positive Control	Ref.
19-Hydroxypenitrem E (94)	Cytotoxicity	Brine shrimp lethality / <i>Artemia salina</i>	4.6 µM (LD ₅₀)	Colchicine 10.7 µM (LD ₅₀)	[38]
	Antibacterial	Well diffusion / <i>Escherichia coli</i>	64.0 µg/mL (MIC)	Chloramphenicol 2.0 µg/mL (MIC)	[38]
		Well diffusion / <i>Edwardsiella tarda</i>	64.0 µg/mL (MIC)	Chloramphenicol 16.0 µg/mL (MIC)	[38]
Penitrem A (95)	Cytotoxicity	Brine shrimp lethality / <i>Artemia salina</i>	1.7 µM (LD ₅₀)	Colchicine 10.7 µM (LD ₅₀)	[38]
	Antibacterial	Well diffusion / <i>Escherichia coli</i>	16.0 µg/mL (MIC)	Chloramphenicol 2.0 µg/mL (MIC)	[38]
		Well diffusion / <i>Edwardsiella tarda</i>	16.0 µg/mL (MIC)	Chloramphenicol 16.0 µg/mL (MIC)	[38]
		Well diffusion / <i>S. aureus</i>	16.0 µg/mL (MIC)	Chloramphenicol 2.0 µg/mL (MIC)	[38]
		Well diffusion / <i>Vibrio anguillarum</i>	16.0 µg/mL (MIC)	Chloramphenicol 0.5 µg/mL (MIC)	[38]
Penijanthe A (96)	Cytotoxicity	Brine shrimp lethality / <i>Artemia salina</i>	8.7 µM (LD ₅₀)	Colchicine 10.7 µM (LD ₅₀)	[38]
Aspernidine G (103)	Cytotoxicity	MTT/HL-60	28.75 µM (IC ₅₀)	<i>cis</i> -platin 3.22 µM (IC ₅₀)	[33]
		MTT/MCF-7	28.31 µM (IC ₅₀)	<i>cis</i> -platin 22.96 µM (IC ₅₀)	[33]
		MTT/SW-480	21.67 µM (IC ₅₀)	<i>cis</i> platin 18.01 µM (IC ₅₀)	[33]
Aspernidine H (104)	Cytotoxicity	MTT/HL-60	15.81 µM (IC ₅₀)	<i>cis</i> -platin 3.22 µM (IC ₅₀)	[33]
		MTT/A-549	33.03 µM (IC ₅₀)	<i>cis</i> -platin 13.17 µM (IC ₅₀)	[33]
		MTT/SMMC-7721	17.17 µM (IC ₅₀)	<i>cis</i> -platin 12.65 µM (IC ₅₀)	[33]
		MTT/MCF-7	17.80 µM (IC ₅₀)	<i>cis</i> -platin 22.96 µM (IC ₅₀)	[33]
		MTT/SW-480	4.77 µM (IC ₅₀)	<i>cis</i> -platin 18.01 µM (IC ₅₀)	[33]
Emeriphenolicin E (108)	Cytotoxicity	SRB/HeLa	4.77 µM (IC ₅₀)	Adriamycin	[39]
		SRB/A549	12.04 µM (IC ₅₀)	Adriamycin	[39]
		SRB/HCT-116	33.05 µM (IC ₅₀)	Adriamycin	[39]
Niduterpenoid A (136)	ERα inhibitors	MCF-7/MTT	11.42 µM (IC ₅₀)	-	[40]
(7Z,9Z,17Z)-2α,3β-dihydroxypregna-7,9,17(20)-trien-18-al (145)	Cytotoxicity	MTT/PC12	7.34 µM (IC ₅₀)	Doxorubicin 5.71 µM (IC ₅₀)	[41]
Microperfurane (173)	Antimicrobial	Serial dilution / <i>Colletotrichum gloeosporioides</i>	32.0 µg/mL (MIC)	Amphotericin B 0.5 µg/mL (MIC)	[31]
		Serial dilution / <i>Edwardsiella ictarda</i>	4.0 µg/mL (MIC)	Chloramphenicol 2.0 µg/mL (MIC)	[31]
		Serial dilution / <i>Edwardsiella tarda</i>	32.0 µg/mL (MIC)	Chloramphenicol 0.5 µg/mL (MIC)	[31]
		Serial dilution / <i>Escherichia coli</i>	32.0 µg/mL (MIC)	Chloramphenicol 1.0 µg/mL (MIC)	[31]
		Serial dilution / <i>Vibrio harvey</i>	16.0 µg/mL (MIC)	Chloramphenicol 1.0 µg/mL (MIC)	[31]
		Serial dilution / <i>Vibrio parahaemolyticus</i>	32.0 µg/mL (MIC)	Chloramphenicol 0.5 µg/mL (MIC)	[31]
9-Hydroxymicroperfurane (174)	Antimicrobial	Serial dilution / <i>Colletotrichum gloeosporioides</i>	64.0 µg/mL (MIC)	Amphotericin B 0.5 µg/mL (MIC)	[31]
		Serial dilution / <i>Edwardsiella tarda</i>	32.0 µg/mL (MIC)	Chloramphenicol 0.5 µg/mL (MIC)	[31]
		Serial dilution / <i>Escherichia coli</i>	64.0 µg/mL (MIC)	Chloramphenicol 1.0 µg/mL (MIC)	[31]
		Serial dilution / <i>Vibrio harvey</i>	16.0 µg/mL (MIC)	Chloramphenicol 1.0 µg/mL (MIC)	[31]
Curvularin (189)	Antimicrobial	Serial dilution / <i>Edwardsiella ictarda</i>	32.0 µg/mL (MIC)	Chloramphenicol 2.0 µg/mL (MIC)	[31]
6-((S,3E,5E)-5,7-Dimethyl-2-oxonona-3,5-dien-1-yl)-2,4-dihydroxy-3-methylbenzaldehyde (202)	Lipoxygenase-1 inhibition	Spectrophotometric / Soybean lipoxygenase 1	97.2 µM (IC ₅₀)	-	[42]

Table 1. Cont.

Compound Name	Biological Activity	Assay, Organism or Cell Line	Biological Results		Ref.
			Compound	Positive Control	
Lecanoric acid (203)	Antimicrobial	Serial dilution/ <i>Aeromonas hydrophilia</i>	32.0 µg/mL (MIC)	Chloramphenicol 0.5 µg/mL (MIC)	[31]
		Serial dilution/ <i>Edwardsiella ictarda</i>	32.0 µg/mL (MIC)	Chloramphenicol 2.0 µg/mL (MIC)	[31]
		Serial dilution/ <i>Escherichia coli</i>	16.0 µg/mL (MIC)	Chloramphenicol 1.0 µg/mL (MIC)	[31]
		Serial dilution/ <i>Vibrio harvey</i>	8.0 µg/mL (MIC)	Chloramphenicol 1.0 µg/mL (MIC)	[31]
		Serial dilution/ <i>Vibrio parahaemolyticus</i>	4.0 µg/mL (MIC)	Chloramphenicol 0.5 µg/mL (MIC)	[31]
Asperoxide A (206)	Antimicrobial	Serial dilution/ <i>Aeromonas hydrophilia</i>	32.0 µg/mL (MIC)	Chloramphenicol 0.5 µg/mL (MIC)	[31]
		Serial dilution/ <i>Edwardsiella tarda</i>	16.0 µg/mL (MIC)	Chloramphenicol 0.5 µg/mL (MIC)	[31]
		Serial dilution/ <i>Vibrio harvey</i>	32.0 µg/mL (MIC)	Chloramphenicol 1.0 µg/mL (MIC)	[31]
		Serial dilution/ <i>Vibrio parahaemolyticus</i>	64.0 µg/mL (MIC)	Chloramphenicol 0.5 µg/mL (MIC)	[31]

3.1. Benzophenones

A. nidulans and its teleomorph *Emericella nidulans* are known to biosynthesize prenylated structurally related benzophenones [43–45]. Many investigations remarked upon the separation of arugosins, which are interesting fungal metabolites that involve the biosynthesis of structurally related polyketides (e.g., anthraquinones, anthrones, xanthenes) (Table 2) [31,43–46].

Table 2. Benzophenones reported from *Aspergillus nidulans*.

Compound Name	Mol. Wt. *	Mol. Formula *	Host (Part, Family)/Location	Ref.
Monodictyphenone (1)	288	C ₁₅ H ₁₂ O ₆	Cultured	[44]
Arugosin F (2)	272	C ₁₅ H ₁₂ O ₅	Cultured	[45]
Arugosin H (3)	356	C ₂₀ H ₂₀ O ₆	Cultured	[45]
	-	-	Green alga, Sardinia, Italy, Mediterranean Sea	[43]
Arugosin I (4)	340	C ₂₀ H ₂₀ O ₅	Cultured	[45]
Nidulalin B (5)	302	C ₁₆ H ₁₄ O ₆	Cultured	[46]
1(3H)-Isobenzofuranone, 3-(2,6-dihydroxyphenyl)-4-hydroxy-6-methyl (6)	272	C ₁₅ H ₁₂ O ₅	Cultured	[44]
Arugosin A (7)	424	C ₂₅ H ₂₈ O ₆	Cultured	[45]
	-	-	Green alga, Sardinia, Italy, Mediterranean Sea	[43]
Arugosin B (8)	424	C ₂₅ H ₂₈ O ₆	Cultured	[45]
	-	-	Green alga, Sardinia, Italy, Mediterranean Sea	[43]
Arugosin C (9)	426	C ₂₅ H ₃₀ O ₆	Deep-sea sediment, South China Sea	[31]
Arugosin G (10)	492	C ₃₀ H ₃₆ O ₆	Green alga, Sardinia, Italy, Mediterranean Sea	[43]

* Mol. Wt.: Molecular weight; Mol. Formula: Molecular formula.

The fungus *E. nidulans* var. *acristata*, isolated from a Mediterranean green alga, yielded two new benzophenones, arugosins G (10) and H (3), together with arugosins A (7) and B (8) that were separated from the EtOAc extract by Sephadex LH-20/HPLC (Figure 1). These metabolites featured prenyl moieties that are connected to the skeleton via an ether linkage.

Compound **3** had antifungal and antialgal potential (IZDs 2 and 3 mm, respectively) vs. *Mycotypha microspora* and *Chlorella fusca*, respectively, whereas **7** and **8** (mixture) revealed antibacterial influence vs. *Bacillus megaterium* (IZD 4 mm) in the agar diffusion assay [43]. Additionally, **7** and **8** demonstrated modest antitumor effectiveness vs. individual cancer cell lines [43]. It is noteworthy that arugosins A (**7**) and B (**8**), dibenz[b,e]oxepin metabolites that were formerly reported from *A. silvaticus*, *A. rugulosus*, and *A. varicolor*, and arugosins C and F were obtained from *Aspergillus* spp. and *Ascodesmis sphaerospora*, respectively [43].

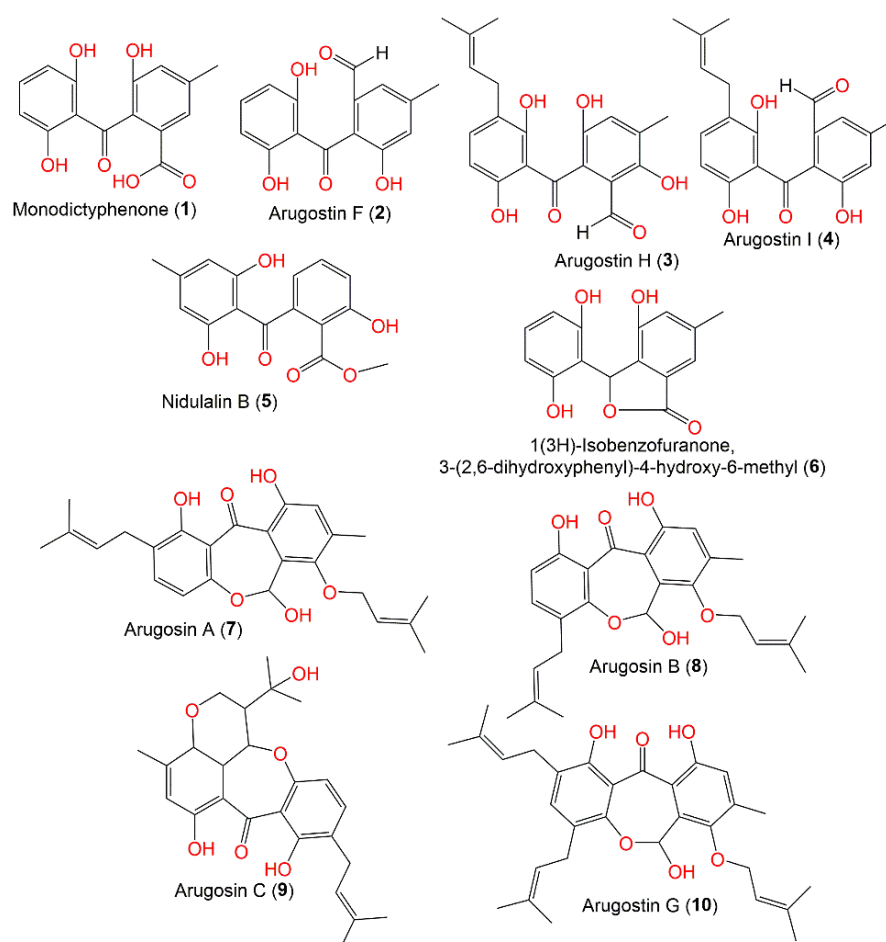
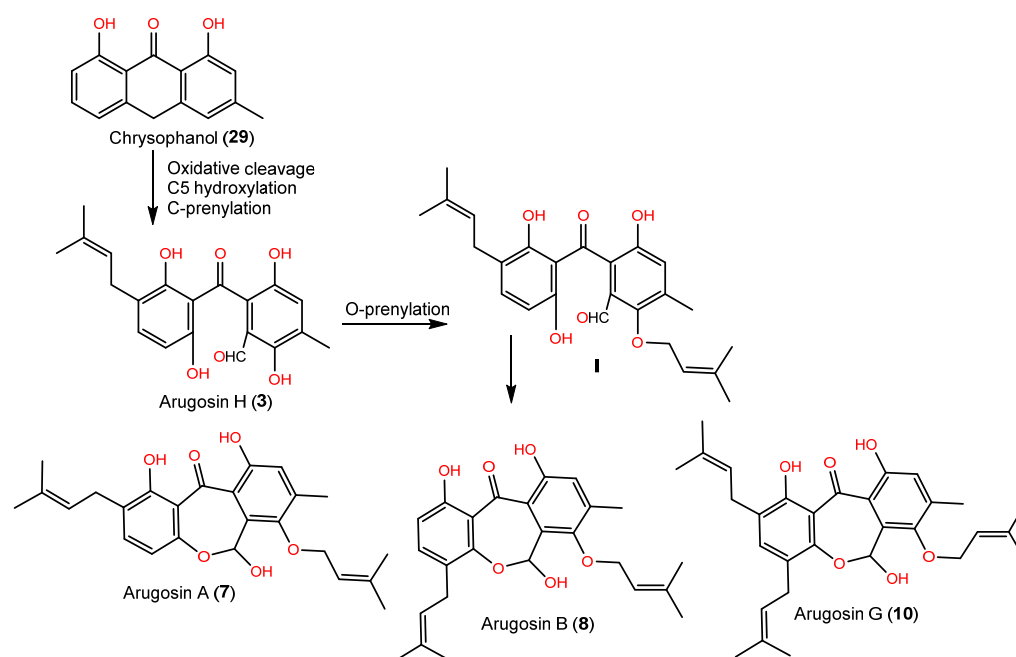


Figure 1. Structures of benzophenones (**1–10**) reported from *Aspergillus nidulans*.

Arugosin H (**3**) was proposed as originating from chrysophanol (**29**, anthrone), which performs oxidative cleavage to produce the aldehyde group, which subsequently undergoes hydroxylation and C-prenylation (Scheme 1). Further, the aldehyde group is converted to a hemiacetal function to produce tricyclic and prenylated metabolites **7**, **8**, and **10** [43].

3.2. Xanthenes and Quinones

Xanthenes are dibenzo- γ -pyrone derivatives that differ in the substituents on the benzene rings, relying on modification reactions and biosynthetic origins. Fungal xanthenes are polyketides created mainly from acetate units and commonly contain a CH_3 group. It was reported that *A. nidulans* produces prenylated xanthenes with varied structures.



Scheme 1. Biosynthetic pathways of compounds 3, 7, 8, and 10 from chrysophanol (29) [43].

Compounds **14**, **16**, and **18** are xanthenes reported from green alga-derived *E. nidulans* var. *acristata* (Table 3). Among them, **18** had antifungal and antialgal capacity (IZDs 11 and 5 mm, respectively) vs. *M. microspora* and *C. fusca*. However, none of them exhibited immune-stimulatory potential against cytokine induction in PBMCs [43]. Compounds **14** and **18** were reported from *A. nidulans* and isolated from Red Sea brown alga, *Turbinaria elatensis*, using SiO₂ and Sephadex LH-20 CC. They had mild inhibition capacity on HCV NS3/4A protease (IC₅₀s 48.5 and 50.0 µg/mL, respectively), compared to HCV-12 (IC₅₀ 1.5 µg/mL) [47]. In 2018, isosecosterigmatocystin (**15**), a new xanthone, in addition to **18**, was separated and identified from the EtOAc culture extract of *A. nidulans* MA-143 under 0.1% ethanol stress. Compound **15** was assigned as having 2'S/3'S based on X-ray analysis [30].

Table 3. Xanthenes and quinones reported from *Aspergillus nidulans*.

Compound Name/Chemical Class	Mol. Wt. *	Mol. Formula *	Host (Part, Family)/Location	Ref.
Xanthenes				
9H-Xanthen-9-one, 8-hydroxy-1-(hydroxymethyl)-3-methyl (11)	256	C ₁₅ H ₁₂ O ₄	Cultured	[44]
Variecoxanthone A (12)	340	C ₂₀ H ₂₀ O ₅	Cultured	[44,45]
Paeciloxanthone (13)	324	C ₂₀ H ₂₀ O ₄	Cultured	[44]
Emericellin (14)	408	C ₂₅ H ₂₈ O ₅	Cultured	[44,45,48,49]
	-	-	Green alga, Sardinia, Italy, Mediterranean Sea	[43]
	-	-	<i>Turbinaria elatensis</i> (Brown alga, <i>Phaeophyceae</i>), Egyptian Red Sea, Ras Mohamed, South Sina, Egypt	[47,50]
Isosecosterigmatocystin (15)	362	C ₁₈ H ₁₈ O ₈	<i>Rhizophora stylosa</i> (Mangrove plant fresh leaves, <i>Rhizophoraceae</i>)	[30]
	-	-	Deep-sea sediment, South China Sea	[31]

Table 3. Cont.

Compound Name/Chemical Class	Mol. Wt. *	Mol. Formula *	Host (Part, Family)/Location	Ref.
Shamixanthone (16)	406	C ₂₅ H ₂₆ O ₅	Cultured	[44,45,48,49]
	-	-	Green alga, Sardinia, Italy, Mediterranean Sea	[43]
	-	-	<i>Turbinaria elatensis</i> (Brown alga, <i>Phaeophyceae</i>), Egyptian Red Sea, Ras Mohamed, South Sina, Egypt	[50]
Epishamixanthone (17)	406	C ₂₅ H ₂₆ O ₅	Cultured	[44,45,49]
Sterigmatocystin (18)	324	C ₁₈ H ₁₂ O ₆	Cultured	[48,49,51]
	-	-	Green alga, Sardinia, Italy, Mediterranean Sea	[43]
	-	-	Soil, Hell Valley, Noboribetsu, Hokkaido, Japan	[52]
	-	-	<i>Rhizophora stylosa</i> (Mangrove plant fresh leaves, <i>Rhizophoraceae</i>)	[30]
	-	-	Deep-sea sediment, South China Sea	[31]
	-	-	<i>Turbinaria elatensis</i> (Brown alga, <i>Phaeophyceae</i>), Egyptian Red Sea, Ras Mohamed, South Sina, Egypt	[47]
	-	-	<i>Nyctanthes arbor-tristis</i> (<i>Oleaceae</i>), Sabira	[53]
Demethylsterigmatocystin (19)	310	C ₁₇ H ₁₀ O ₆	Cultured	[54]
1-Hydroxy-3-methylxanthone (20)	226	C ₁₄ H ₁₀ O ₃	<i>Nyctanthes arbor-tristis</i> (<i>Oleaceae</i>), Sabira	[53]
Nidulalin A (21)	302	C ₁₆ H ₁₄ O ₆	Cultured	[46]
Quinones				
1,6,8-Trihydroxyxanthone (22)	256	C ₁₄ H ₈ O ₅	Cultured	[55]
Emodin (23)	270	C ₁₅ H ₁₀ O ₅	Cultured	[44,55]
2-Hydroxyemodin (24)	286	C ₁₅ H ₁₀ O ₆	Cultured	[56]
2,ω-Dihydroxyemodin (25)	302	C ₁₅ H ₁₀ O ₇	Cultured	[44]
ω-Hydroxyemodin (26)	286	C ₁₅ H ₁₀ O ₆	Cultured	[44]
Aloe-emodin (27)	270	C ₁₅ H ₁₀ O ₅	Cultured	[44]
Endocrocin (28)	314	C ₁₆ H ₁₀ O ₇	Cultured	[44]
Chrysophanol (29)	254	C ₁₅ H ₁₀ O ₄	Cultured	[44,45]
Asperthecin (30)	318	C ₁₅ H ₁₀ O ₈	Cultured	[49,57]
3'-Hydroxyversiconol (31)	376	C ₁₈ H ₁₆ O ₉	Cultured	[54]
Versiconol (32)	360	C ₁₈ H ₁₆ O ₈	Cultured	[56]
Averantin (33)	372	C ₂₀ H ₂₀ O ₇	Cultured	[56]
Norsolorinic acid (34)	370	C ₂₀ H ₁₈ O ₇	Cultured	[55]
	-	-	<i>Rhizophora stylosa</i> (Mangrove plant fresh leaves, <i>Rhizophoraceae</i>)	[30]
Versicolorin C (35)	340	C ₁₈ H ₁₂ O ₇	Cultured	[48,51]
	-	-	<i>Rhizophora stylosa</i> (Mangrove plant fresh leaves, <i>Rhizophoraceae</i>)	[30]
Isoversicolorin C (36)	340	C ₁₈ H ₁₂ O ₇	<i>Rhizophora stylosa</i> (Mangrove plant fresh leaves, <i>Rhizophoraceae</i>)	[30]
8-O-Methylversicolorin A (37)	352	C ₁₉ H ₁₂ O ₇	Deep-sea sediment, western Pacific Ocean, China	[58]

Table 3. Cont.

Compound Name/Chemical Class	Mol. Wt. *	Mol. Formula *	Host (Part, Family)/Location	Ref.
Aversin (38)	368	C ₂₀ H ₁₆ O ₇	Deep-sea sediment, western Pacific Ocean, China	[58]
Averufin (39)	368	C ₂₀ H ₁₆ O ₇	Cultured <i>Rhizophora stylosa</i> (Mangrove plant fresh leaves, <i>Rhizophoraceae</i>)	[48,51] [30]
6-O-Methylaverufin (40)	382	C ₂₁ H ₁₈ O ₇	Deep-sea sediment, western Pacific Ocean, China	[58]
6,8-Di-O-Methylaverufin (41)	396	C ₂₂ H ₂₀ O ₇	Deep-sea sediment, western Pacific Ocean, China	[58]
Nidurufin (42)	384	C ₂₀ H ₁₆ O ₈	Cultured	[51]
Ascoquinone A (43)	618	C ₃₀ H ₁₈ O ₁₅	Cultured	[55]
Averufanin (44)	370	C ₂₀ H ₁₈ O ₇	<i>Rhizophora stylosa</i> (Mangrove plant fresh leaves, <i>Rhizophoraceae</i>)	[30]
Paeciloxanthone E (45)	368	C ₂₀ H ₁₆ O ₇	<i>Rhizophora stylosa</i> (Mangrove plant fresh leaves, <i>Rhizophoraceae</i>)	[30]
<i>cis</i> -Emodinphysicon-bianthrone (46)	524	C ₃₁ H ₂₄ O ₈	Cultured	[56]
<i>trans</i> -Emodin-physicon-bianthrone (47)	524	C ₃₁ H ₂₄ O ₈	Cultured	[56]

* Mol. Wt.: Molecular weight; Mol. Formula: Molecular formula.

The cytotoxic capacity of **18** and **20** vs. NCI-H460, MCF-7, and HeLa cell lines in the SRB was assessed. Only **18** (IC₅₀ 50 µM/mL) possessed growth inhibition capacity vs. the MCF-7 cell, whereas **20** was inactive (IC₅₀ > 100) [53] (Figure 2).

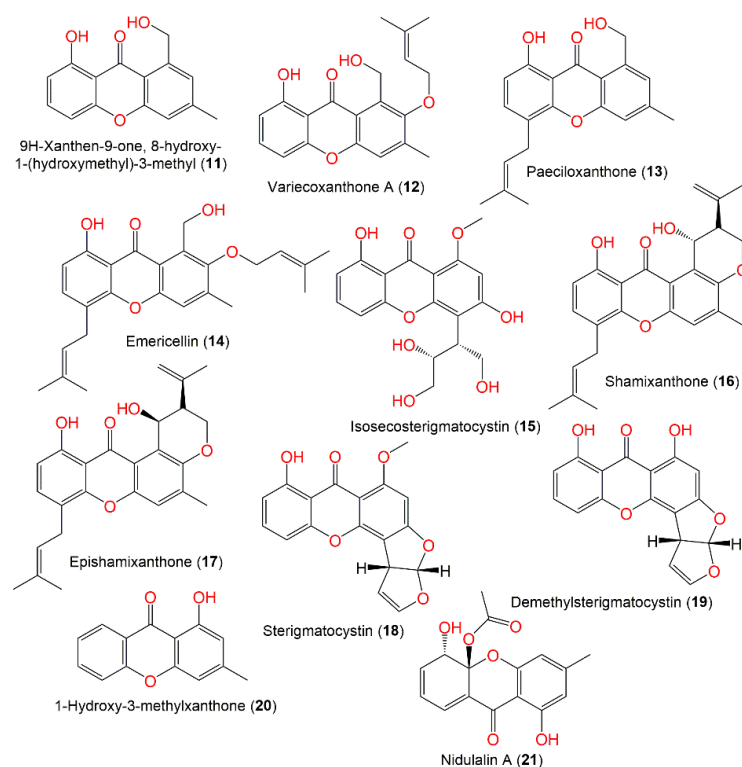
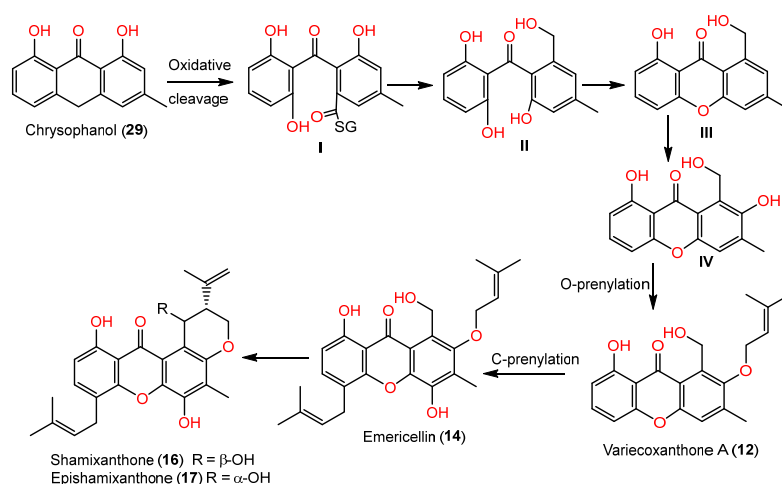


Figure 2. Structures of xanthonones (11–21) reported from *Aspergillus nidulans*.

Also, the xanthones were proposed to be biosynthesized from **29**, which is transformed by quinone ring oxidative cleavage into thiolester **I**. Its oxidoreductase-catalyzed reduction yields benzophenone alcohol (**II**). The alcohol (**II**) produces 1-hydroxy-6-methyl-8-hydroxymethylxanthone (**III**) via H_2O elimination, and then hydroxylation via monooxygenase produces 1,7-dihydroxy-6-methyl-8-hydroxymethylxanthone (**IV**). The latter's prenyltransferase-catalyzed prenylation results in **12**, which is C-prenylated to form **14**. Subsequent cyclization of **14** produces **16** and **17** (Scheme 2) [45].



Scheme 2. Biosynthetic pathways of **12**, **14**, **16**, and **17** [45].

Nidurufin (**42**), a new metabolite of which is hydroxyaverufin, and **39** were purified from the $CHCl_3$:MeOH extract of *A. nidulans* G-106 using silica and formamide-impregnated cellulose powder and characterized by spectral and chemical methods (Figure 3) [51].

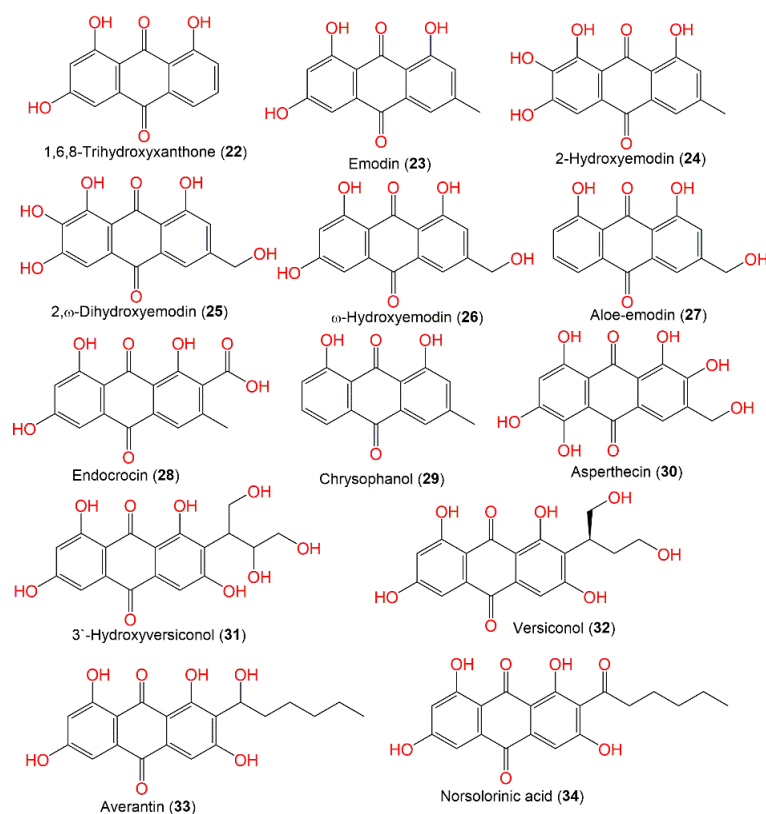


Figure 3. Structures of quinones (**22**–**34**).

The aggregation of the microtubule-accompanied protein *tau* is substantial in various neurodegenerative illnesses, such as Alzheimer's disease. Interestingly, **25** and **30** demonstrated potent *tau* aggregation inhibition potential, which was observed in a filter trap assay and by electron microscopy. In addition, **25** and **30** lessened *tau* aggregation without blocking *tau* stabilization of microtubules, like **23**.

Together, these metabolites demonstrated potential as lead compounds for developing *tau* aggregation inhibitors in Alzheimer's disease and neurodegenerative tauopathies [54]. Isoversicolorin C (**36**), a new anthraquinone derivative, and six related metabolites—**34**, **35**, **39**, **45**, and **44**—were purified and characterized from the EtOAc culture extract of mangrove-derived *A. nidulans* MA-143 under ethanol 0.1% stress (Figure 4). Their isolation and elucidation were accomplished by SiO₂/RP-18/Sephadex LH-20 and NMR/ECD/X-ray. Compound **36** had potent antibacterial capacity vs. *E. ictaluri* and *V. alginolyticus* (MICs 4.0 and 1.0 µg/mL, respectively); however, **35** possessed capacity vs. *M. luteus*, *E. coli*, *V. parahaemolyticus*, *V. alginolyticus*, and *E. ictaluri* (MICs ranged from 1.0 to 8.0 µg/mL), which were comparable to chloramphenicol [30].

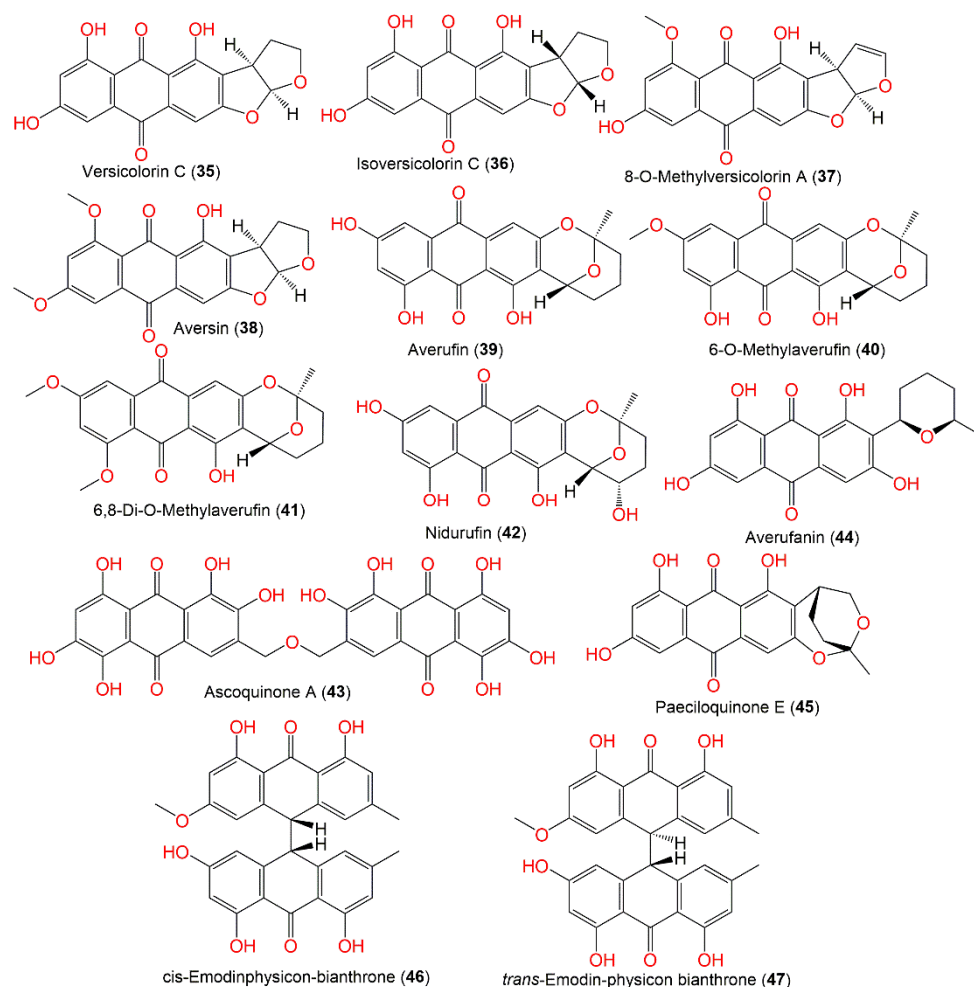


Figure 4. Structures of quinones (**35–47**).

3.3. Depsidones and Biphenyl Ethers

Depsidones consist of two 2,4-dihydroxy-benzoic acid moieties, connecting via ester and ether bonds, resulting in 11H-dibenzo[b,e] [1,4] dioxepin-11-one core formation [59]. They originated from depsides' direct-oxidative coupling of the A 2OH ring and the B 5' carbon ring. These metabolites were found to have diversified potential: anti-malarial, herbicidal, anti-leishmanial, larvicidal, antifungal, cholinesterase and aromatase inhibitory, and antioxidant activity [59].

Compounds **48** and **49** were separated from the *A. nidulans* mycelia's light petroleum ether extract by repeated crystallization from the EtOH and petroleum ether (Table 4). Compound **48** is a monomethyl ether that completely suppressed *Mycobacterium tuberculosis* growth for 4 weeks, as well as *Microsporum audouini* and *Trichophyton tonsurans*, and was inactive against bacteriophages [60].

Table 4. Depsidone and diphenyl ethers reported from *Aspergillus nidulans*.

Compound Name/ Chemical Class	Mol. Wt. *	Mol. Formula *	Host (Part, Family)/Location	Ref.
Depsidone				
Nidulin (48)	443	C ₂₀ H ₁₇ Cl ₃ O ₅	Cultured	[60]
Nor-nidulin (Ustin) (49)	427	C ₁₉ H ₁₅ Cl ₃ O ₅	Cultured	[60]
Dechloro-nornidulin (50)	394	C ₁₉ H ₁₆ Cl ₂ O ₅	Cultured	[61]
Trisdechloro-nornidulin (51)	326	C ₁₉ H ₁₈ O ₅	Cultured	[61]
Diphenyl ethers				
Violaceol I (52)	262	C ₁₄ H ₁₄ O ₅	Cultured	[32]
Violaceol II (53)	262	C ₁₄ H ₁₄ O ₅	Cultured	[32]
Diorcinol (54)	230	C ₁₄ H ₁₄ O ₃	Cultured	[32]
	-	-	Soil, Hell Valley, Noboribetsu, Hokkaido, Japan	[52]
	-	-	Deep-sea sediment, western Pacific Ocean, China	[58]
Cordylol C (55)	246	C ₁₄ H ₁₄ O ₄	Cultured	[32]
Gibellulin A (56)	360	C ₁₄ H ₁₂ O ₅	Deep-sea sediment, South China Sea	[31]
Gibellulin C (57)	274	C ₁₅ H ₁₄ O ₅	Cultured	[57]
Gibellulin D (58)	274	C ₁₅ H ₁₄ O ₅	Cultured	[57]
F9775 A (59)	396	C ₂₁ H ₁₆ O ₈	Cultured	[54]
F9775 B (60)	396	C ₂₁ H ₁₆ O ₈	Cultured	[54]

* Mol. Wt.: Molecular weight; Mol. Formula: Molecular formula.

The co-culture of *A. nidulans* and *A. fumigatus* enhanced the production of diphenyl ethers, **52–55**, which were separated by SiO₂ CC/HPLC and identified by NMR tools (Figure 5). These metabolites (**52–55**) possessed antibacterial potential against *B. subtilis* (MICs 6.3–100 µg/mL) compared to chloramphenicol, indicating that the hydroxylation enhanced the antibacterial effect of diphenyl ethers [32]. In addition, **56** revealed potent antimicrobial effectiveness (MICs 2–4 µg/mL) vs. *E. ictarda*, *A. hydrophilia*, *E. tarda*, and *V. harveyi* (aquatic pathogens) and *C. gloeosporioides* (pathogenic plant fungus), which could be further studied in terms of developing antimicrobial agents [31].

3.4. Alkaloids

3.4.1. Quinolone Alkaloids

Natural quinoline alkaloids are an abundant class of alkaloids that have been reported as having animal, plant, and microbial origins. Some investigations remarked upon the separation of quinoline alkaloids from *A. nidulans*.

A combined analytical and genomic approach and metabolic investigation of *A. nidulans* HKI 0410 under various culture conditions resulted in aspoquinolones A–D (**61–64**), which were separated utilizing SiO₂/Sephadex LH-20/HPLC and assigned by NMR [62]. Compounds **61** and **62** are isomers with 3-methoxy-4,6-dihydroxy-4-(4'-methoxyphenyl) quinolinone and unusual 2,2,4-trimethyl-3-oxa-bicyclo[3.1.0]hexane moieties; however, **63** and **64** are diastereomers (ratio 2:1) sharing the same 3-methoxy-4,6-dihydroxy-4-

(4'-methoxyphenyl)quinolinone skeleton as **61** and **62** (Figure 6; Table 5). Compounds **61** and **62** exhibited remarkable cytotoxic and antiproliferative capacity on L-929 (GI₅₀ 10.6/11.4 µg/mL) and K-562 (GI₅₀ 17.8/21.2 µg/mL) cell lines, respectively.

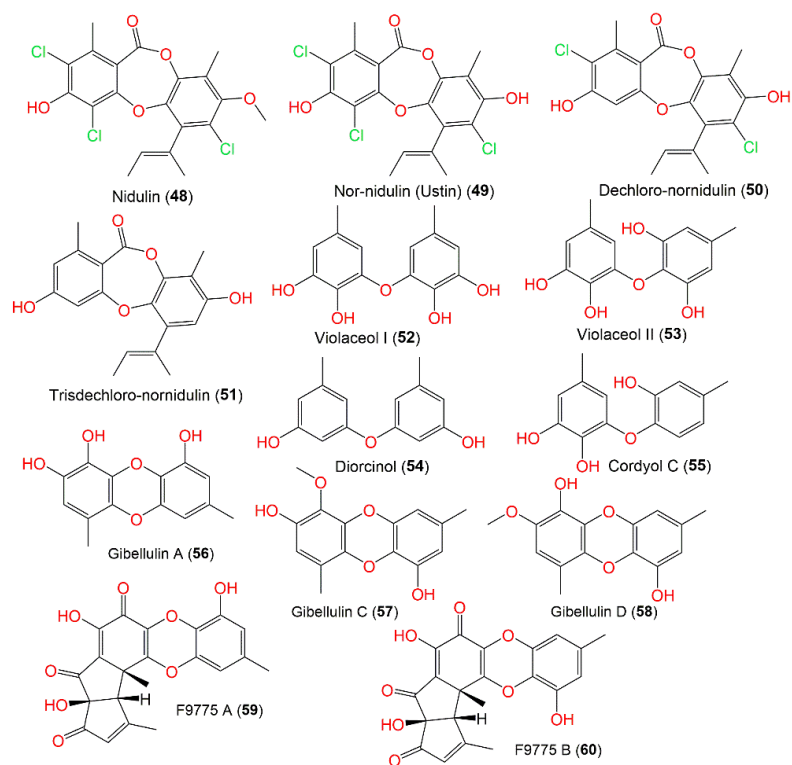


Figure 5. Structures of depsidones (**48–51**) and biphenyl ethers (**52–60**).

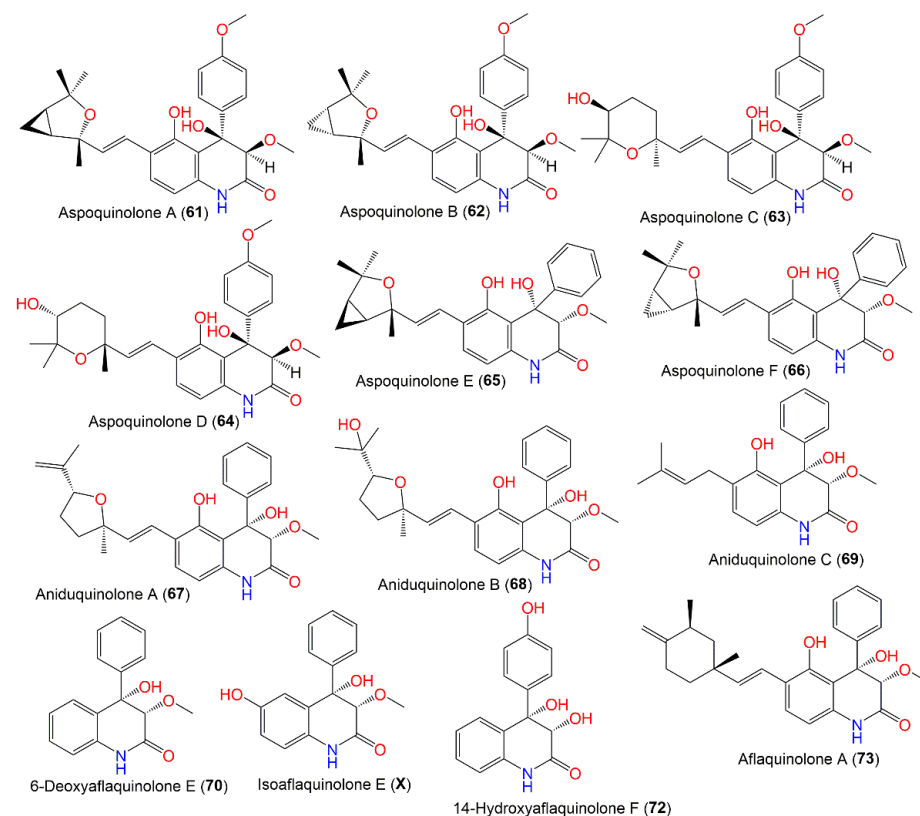


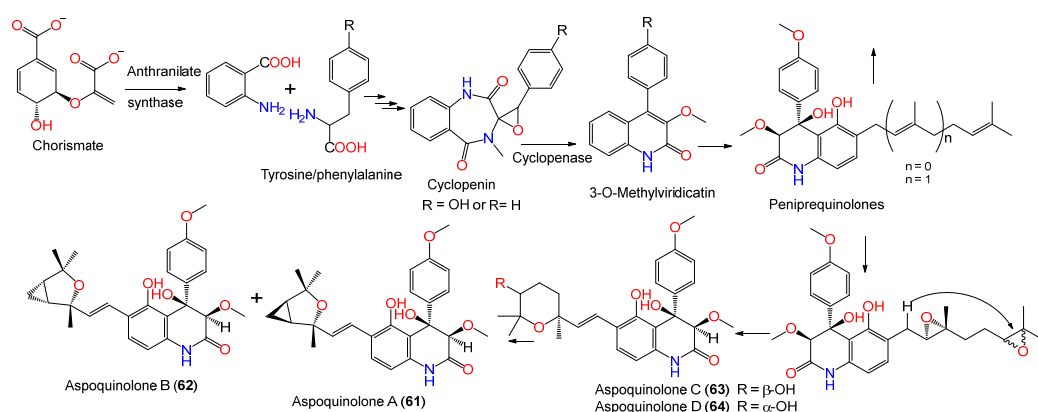
Figure 6. Structures of quinoline alkaloids (**61–73**).

Table 5. Quinoline alkaloids reported from *Aspergillus nidulans*.

Compound Name	Mol. Wt. *	Mol. Formula *	Host (Part, Family)/Location	Ref.
Aspoquinolone A (61)	465	C ₂₇ H ₃₁ NO ₆	Cultured	[62]
Aspoquinolone B (62)	465	C ₂₇ H ₃₁ NO ₆	Cultured	[62]
Aspoquinolone C (63)	483	C ₂₇ H ₃₃ NO ₇	Cultured	[62]
Aspoquinolone D (64)	483	C ₂₇ H ₃₃ NO ₇	Cultured	[62]
Aspoquinolone E (65)	435	C ₂₆ H ₂₉ NO ₅	<i>Whitmania pigra</i> (Annelida, segmented worm, <i>Hirudinidae</i>), Hubei, China	[33]
Aspoquinolone F (66)	435	C ₂₆ H ₂₉ NO ₅	<i>Whitmania pigra</i> (Annelida, segmented worm, <i>Hirudinidae</i>), Hubei, China	[33]
Aniduquinolone A (67)	435	C ₂₆ H ₂₉ NO ₅	<i>Rhizophora stylosa</i> (Mangrove plant fresh leaves, <i>Rhizophoraceae</i>)	[34]
Aniduquinolone B (68)	453	C ₂₆ H ₃₁ NO ₆	<i>Rhizophora stylosa</i> (Mangrove plant fresh leaves, <i>Rhizophoraceae</i>)	[34]
Aniduquinolone C (69)	353	C ₂₁ H ₂₃ NO ₄	<i>Rhizophora stylosa</i> (Mangrove plant fresh leaves, <i>Rhizophoraceae</i>)	[34]
6-Deoxyaflaquinolone E (70)	269	C ₁₆ H ₁₅ NO ₃	<i>Rhizophora stylosa</i> (Mangrove plant fresh leaves, <i>Rhizophoraceae</i>)	[34]
Isoaflaquinolone E (71)	285	C ₁₆ H ₁₅ NO ₄	<i>Rhizophora stylosa</i> (Mangrove plant fresh leaves, <i>Rhizophoraceae</i>)	[34]
14-Hydroxyaflaquinolone F (72)	271	C ₁₅ H ₁₃ NO ₄	<i>Rhizophora stylosa</i> (Mangrove plant fresh leaves, <i>Rhizophoraceae</i>)	[34]
Aflaquinolone A (73)	433	C ₂₇ H ₃₁ NO ₄	<i>Rhizophora stylosa</i> (Mangrove plant fresh leaves, <i>Rhizophoraceae</i>)	[34]

* Mol. Wt.: Molecular weight; Mol. Formula: Molecular formula.

These metabolites were postulated as originating from cyclophenin (benzodiazepine, I) formed from anthranilic acid and tyrosine/or phenylalanine, which is biosynthesized by anthranilate synthase (Scheme 3). This enzyme catalyzed the conversion of chorismate to anthranilic acid for tryptophan biosynthesis [62].

**Scheme 3.** Biosynthetic pathways of aspoquinolones A–D (61–64) [62].

From Annelida *Whitmania pigra*-associated *A. nidulans*, aspoquinolones E (65) and F (66), new prenylated quinolinone alkaloids were purified utilizing SiO₂/Sephadex LH-20/HPLC. Their configurations and structures were determined based on spectral and ECD analyses. They featured 3S/4S configuration, with an unusual 2,2,4-trimethyl-3-oxa-

bicyclo[3.1.0]hexane moiety. Their cytotoxic evaluation vs. A-549, HL-60, and MCF-7 revealed that **65** exhibited moderate cytotoxic capacity (IC_{50} s 3.50, 29.15, and 24.5 μ M, respectively) compared to *cis*-platin (IC_{50} s 13.17, 3.22, and 22.96 μ M, respectively). It is noteworthy that **65** and **66**, with the same structure but different cyclopropyl ring configuration, were greatly varied in activity, suggesting that the cyclopropyl ring configuration influenced the activity [33].

In 2013, the separation of new 4-phenyl-3,4-dihydroquinolone derivatives, **67–72**, along with known related analog **73**, was reported from a *Rhizophora stylosa*-associated *A. nidulans* MA-143 extract by SiO_2 /RP-18/sephadex LH-20/HPLC. Their structures and absolute configuration were established by spectral, ECD, and X-ray analyses. Compounds **70–72** share with **67–69** the 4-phenyl-3,4-dihydroquinolone moiety but lack the terpenoid side chain, as in **67–69**. Additionally, **67** was related to **73**; however, **67** lacks the cyclohexane moiety in the terpenoid side chain of **73**; instead, it features a terminal double bond and substituted tetrahydrofuran moiety. These metabolites did not have cytotoxic (vs. BEL-7402, MDA-MB-231, HL-60, and K562) or antibacterial (*E. coli* and *S. aureus*) potential in the MTT and well diffusion methods, respectively, while **68**, **69**, and **73** had a marked brine shrimp lethality (LD_{50} 7.1, 4.5, and 5.5 μ M, respectively) that was more powerful than colchicine (LD_{50} 88.4 μ M) [34].

3.4.2. Quinazolinone, Pyrazine, and Dioxopiperazine Alkaloids

Additionally, four new quinazolinone alkaloids, namely aniquinazolines A–D (**74–77**), were also purified from *E. nidulans* using SiO_2 /Sephadex LH-20/HPLC and elucidated by spectral analyses, and their absolute configurations were assigned based on acidic hydrolysate chiral HPLC, ECD, and X-ray analyses (Figure 7). Their configurations are 3R/14R/17R/18R/20S (**74** and **76**), 3R/14R/17R/18R (**75**), and 14R/17S/18S/20S (**77**). Compounds **74–77** had potent brine shrimp lethality (LD_{50} s 1.27–4.95 μ M) compared to colchicine (LD_{50} 88.4 μ M). Unfortunately, they did not have anticancer potential vs. MDA-MB-231, BEL-7402, K562, and HL-60 or antibacterial capacity vs. *E. coli* and *S. aureus* in the MTT and well diffusion assays, respectively [35].

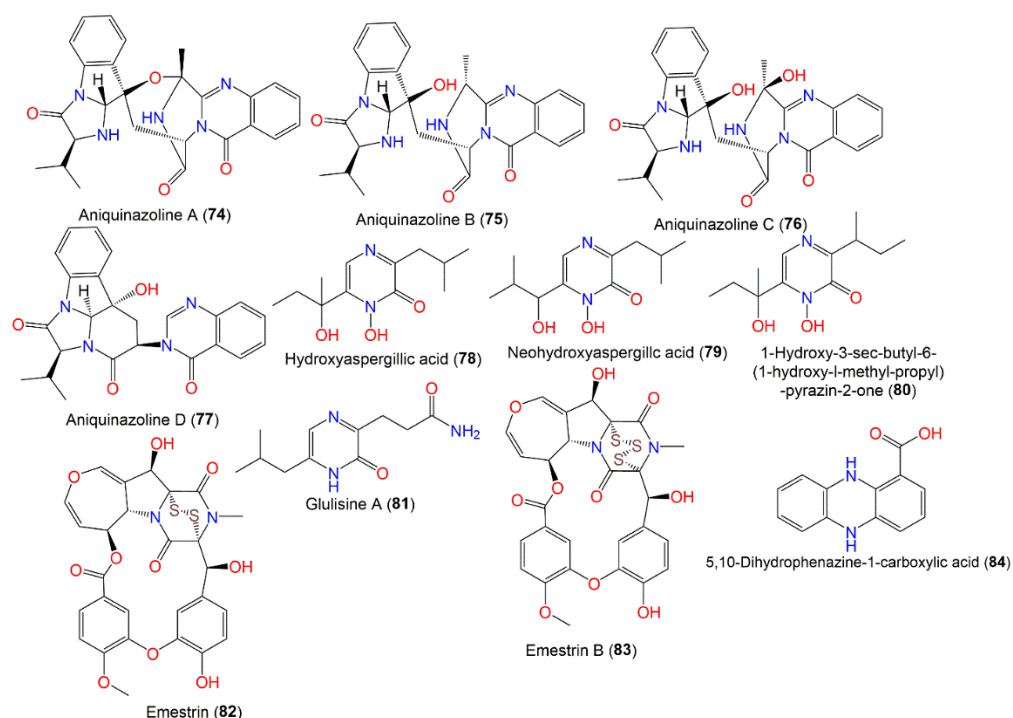


Figure 7. Structures of quinazolinone (**74–77**), pyrazine (**78–81**), dioxopiperazine (**82** and **83**), and phenazine (**84**) alkaloids.

Emestrin (**82**), a six-membered-ring dioxopiperazine with a disulfide bridge, is part of the epipoly-thio-dioxopiperazine family obtained from ascidian *Aplidium longithorax*-associated *E. nidulans* MFW39 and collected from Wakatobi Marine National Park, Indonesia utilizing SiO₂ CC/HPLC (Table 6). It was found to have noticeable cytotoxic potential (IC₅₀s ranged from 1.8 to 13.8 µg/mL) vs. C28, T47D, HeLa, and HepG₂ but was weakly active against Vero cells (IC₅₀ 260.9 µg/mL). Emestrin (Conc. 1.0 µg/mL) caused G₀/G₁ arrest of the cell cycle, and also induced apoptosis (Conc. 1.0 and 3.0 µg/mL) of 83.6 and 92.6%, respectively, on T47D cells. This effect was linked to a disulphide bond and unique epithio-dioxopiperazine moiety [36]. Another epipolythiodioxopiperazine derivative, emestrin B (**83**), was separated from marine-derived *E. nidulans* using SiO₂ CC/preparative TLC and was assessed for cytotoxic capacity in the MTT assay vs. the WiDr, HeLa, and T47D cancer cell lines. It had remarkable cytotoxic influence on IC₅₀s 1.02, 1.56, and 0.16 µg/mL, respectively. This metabolite had apoptotic action against T47D cells (74.1%), compared to doxorubicin (74.8%) [37]. Compound **84**, purified from the *Nyctanthes arbor-tristis*-inhabited fungus strain, had no cytotoxic effectiveness vs. the NCI-H460, MCF-7, and HeLa cell lines in the SRB [53]. Glulisine A (**81**), a new nitrogenous metabolite, was reported from 1% ethanol-stressed *A. nidulans* MA-143. It was assigned by NMR and X-ray analyses as being derived from leucine and glutamine [30].

Table 6. Quinazolinone, pyrazine, dioxopiperazine, and phenazine alkaloids reported from *A. nidulans*.

Compound Name/Chemical Class	Mol. Wt. *	Mol. Formula *	Host (Part, Family)/Location	Ref.
Quinazolinone alkaloids				
Aniquinazoline A (74)	471	C ₂₆ H ₂₅ N ₅ O ₄	<i>Rhizophora stylosa</i> (Mangrove plant fresh leaves, <i>Rhizophoraceae</i>)	[35]
Aniquinazoline B (75)	473	C ₂₆ H ₂₇ N ₅ O ₄	<i>Rhizophora stylosa</i> (Mangrove plant fresh leaves, <i>Rhizophoraceae</i>)	[35]
Aniquinazoline C (76)	489	C ₂₆ H ₂₇ N ₅ O ₅	<i>Rhizophora stylosa</i> (Mangrove plant fresh leaves, <i>Rhizophoraceae</i>)	[35]
Aniquinazoline D (77)	430	C ₂₂ H ₂₄ N ₄ O ₄	<i>Rhizophora stylosa</i> (Mangrove plant fresh leaves, <i>Rhizophoraceae</i>)	[35]
Pyrazine alkaloids				
Hydroxyaspergillic acid (78)	240	C ₁₂ H ₂₀ N ₂ O ₃	Cultured	[63]
Neohydroxyaspergillic acid (79)	240	C ₁₂ H ₂₀ N ₂ O ₃	Cultured	[63]
1-Hydroxy-3-sec-butyl-6-(1-hydroxy-l-methyl-propyl)-pyrazin-2-one (80)	240	C ₁₂ H ₂₀ N ₂ O ₃	Cultured	[63]
Glulisine A (81)	223	C ₁₁ H ₁₇ N ₃ O ₂	<i>Rhizophora stylosa</i> (Mangrove plant fresh leaves, <i>Rhizophoraceae</i>)	[30]
Dioxopiperazine alkaloids				
Emestrin (82)	598	C ₂₇ H ₂₂ N ₂ O ₁₀ S ₂	Soil, Hell Valley, Noboribetsu, Hokkaido, Japan <i>Aplidium longithorax</i> (Ascidin, <i>Polyclinidae</i>), Wakatobi Marine National Park, Southeast Sulawesi, Indonesia	[36,52] [36]
Emestrin B (83)	630	C ₂₇ H ₂₂ N ₂ O ₁₀ S ₃	<i>Aplidium longithorax</i> (Marine Ascidin, <i>Polyclinidae</i>), Wakatobi Marine National Park, Southeast Sulawesi, Indonesia	[37]
Phenazine alkaloids				
5,10-Dihydrophenazine-1-carboxylic acid (84)	226	C ₁₃ H ₁₀ N ₂ O ₂	<i>Nyctanthes arbor-tristis</i> Linn (<i>Oleaceae</i>), Sabira	[53]

* Mol. Wt.: Molecular weight; Mol. Formula: Molecular formula.

3.4.3. Indole Derivatives

The indole alkaloid emindole DA (97), separated from green alga-associated fungus, possessed antitumor potential vs. 36 human tumor cell line panels (mean IC_{50} s 5.5 μ g/mL) in the propidium iodide fluorescence assay [43]. In an antimicrobial assay vs. various aquatic, plant, and human pathogens, terrequinone A (92) exhibited marked efficacy (MIC 2 μ g/mL) vs. *E. coli*, *V. alginolyticus*, and *C. gloeosporioides*, compared to chloramphenicol and amphotericin B, suggesting the potency of 92 as a lead metabolite for antimicrobial agents [31]. Ergotryptamine (87) is an alkaloid produced by an engineered *A. nidulans* WFC that was designated using labeling, MS, and NMR tools. It differs from N-methyl-4-dimethylallyltryptophan (88) by the addition of the OH group, loss of the COOH group, and shifting of the double bond position [64] (Figure 8).

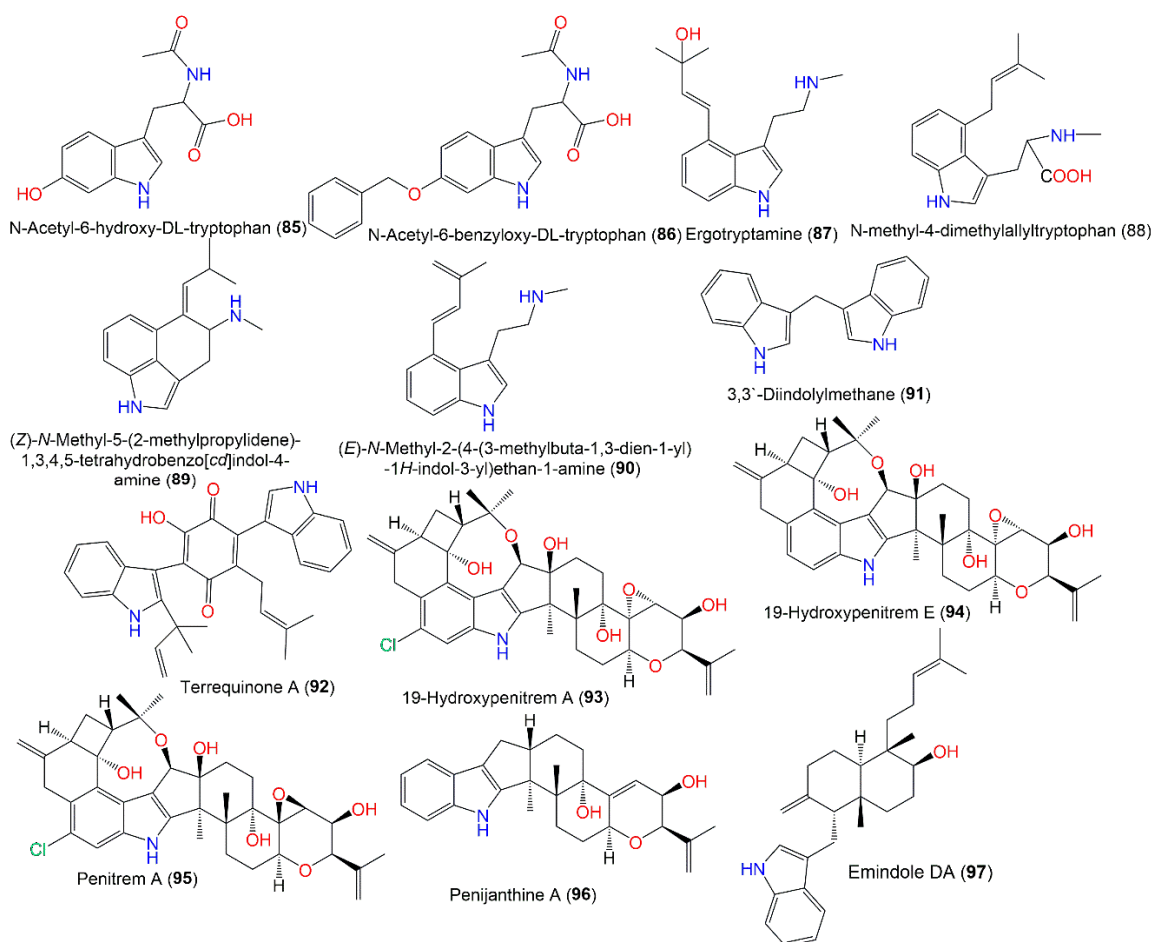


Figure 8. Structures of indole (85–97) alkaloids.

3.4.4. Isoindole Derivatives

The production of new isoindole alkaloids, aspernidine A (99) and B (100 X2), by *A. nidulans* AXB4A2 cultivated in malt medium at increased orbital shaking (200 rpm) and elevated temperature (37 °C) with p-aminobenzoate/uridine supplementation, was reported. These metabolites were separated via SiO_2 /Sephadex LH-20/HPLC and characterized by MS and NMR tools (Figure 9). Compounds 99 and 100 had moderate anti-proliferation potential with respect to L-929 and K-562 (GI_{50} 35.8/34.3 μ M for 99 and 39.5/39.5 μ M for 100, respectively) and weak cytotoxicity with respect to HeLa (CC_{50} 94.0 and 65.5 μ M, respectively) [65] (Table 7).

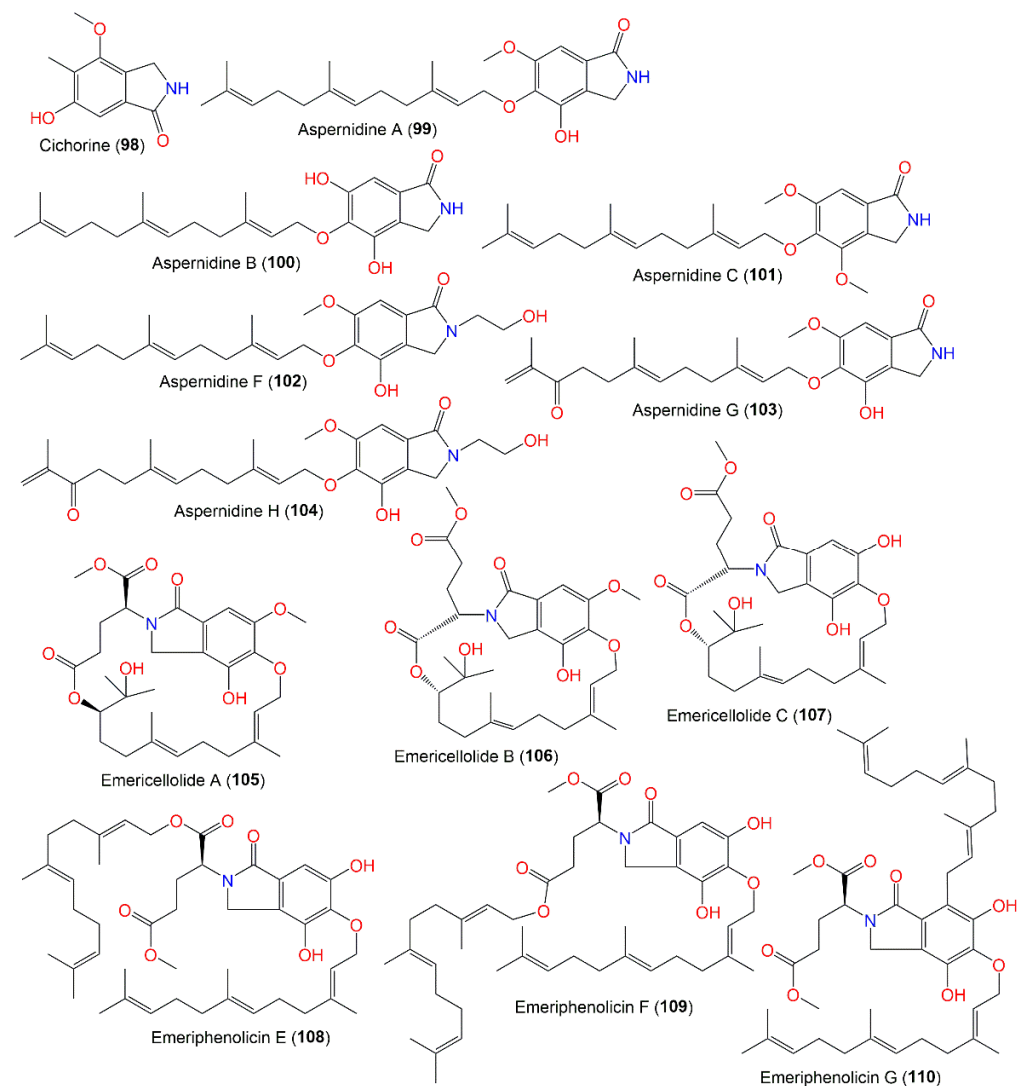


Figure 9. Structures of isoindole (98–110) alkaloids.

Table 7. Indole and isoindole alkaloids reported from *A. nidulans*.

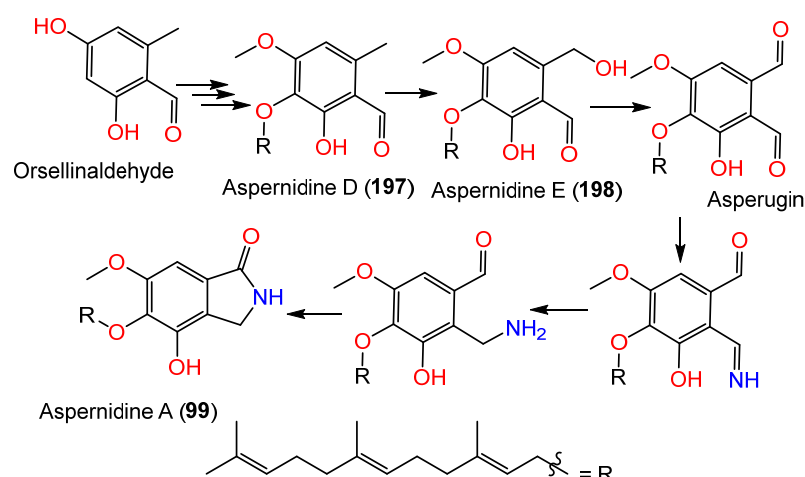
Compound Name/Chemical Class	Mol. Wt. *	Mol. Formula *	Host (Part, Family)/Location	Ref.
Indole alkaloids				
N-Acetyl-6-hydroxy-DL-tryptophan (85)	262	C ₁₃ H ₁₄ N ₂ O ₄	Cultured	[66]
N-Acetyl-6-benzyloxy-DL-tryptophan (86)	352	C ₂₀ H ₂₀ N ₂ O ₄	Cultured	[66]
Ergotryptamine (87)	258	C ₁₆ H ₂₂ N ₂ O	Mutant strain cultured	[64]
N-methyl-4-dimethylallyltryptophan (88)	286	C ₁₇ H ₂₂ N ₂ O ₂	Mutant strain cultured	[64]
(Z)-N-Methyl-5-(2-methylpropylidene)-1,3,4,5-tetrahydrobenzo[cd]indol-4-amine (89)	240	C ₁₆ H ₂₀ N ₂	Mutant strain cultured	[64]
(E)-N-Methyl-2-(4-(3-methylbuta-1,3-dien-1-yl)-1H-indol-3-yl)ethan-1-amine (90)	240	C ₁₆ H ₂₀ N ₂	Mutant strain cultured	[64]
3,3'-Diindolylmethane (91)	246	C ₁₇ H ₃₀ N ₂ O ₃	Deep-sea sediment, South China Sea	[31]

Table 7. Cont.

Compound Name/Chemical Class	Mol. Wt. *	Mol. Formula *	Host (Part, Family)/Location	Ref.
Terrequinone A (92)	490	C ₃₂ H ₃₀ N ₂ O ₃	Deep-sea sediment, South China Sea	[31]
19-Hydroxypenitrem A (93)	649	C ₃₇ H ₄₄ ClNO ₇	<i>Polysiphonia scopulorum</i> var. <i>villum</i> (Red alga, Rhodomelaceae), Yantai, North China	[38]
19-Hydroxypenitrem E (94)	615	C ₃₇ H ₄₅ NO ₇	<i>Polysiphonia scopulorum</i> var. <i>villum</i> (Red alga, Rhodomelaceae), Yantai, North China	[38]
Penitrem A (95)	649	C ₃₇ H ₄₄ ClNO ₇	<i>Polysiphonia scopulorum</i> var. <i>villum</i> (Red alga, Rhodomelaceae), Yantai, North China	[38]
Penijanthine A (96)	419	C ₂₇ H ₃₃ NO ₃	<i>Polysiphonia scopulorum</i> var. <i>villum</i> (Red alga, Rhodomelaceae), Yantai, North China	[38]
Emindole DA (97)	405	C ₂₈ H ₃₉ NO	Green alga, Sardinia, Italy, Mediterranean Sea	[43]
Isoindole alkaloids				
Cichorine (98)	193	C ₁₀ H ₁₁ NO ₃	Cultured	[44,57]
Aspernidine A (99)	399	C ₂₄ H ₃₃ NO ₄	Cultured	[65]
Aspernidine B (100)	385	C ₂₃ H ₃₁ NO ₄	Cultured	[65]
Aspernidine C (101)	413	C ₂₅ H ₃₅ NO ₄	Cultured	[49]
Aspernidine F (102)	443	C ₂₆ H ₃₇ NO ₅	<i>Whitmania pigra</i> (Annelida, segmented worm, Hirudinidae), Hubei, China	[33]
Aspernidine G (103)	413	C ₂₄ H ₃₁ NO ₅	<i>Whitmania pigra</i> (Annelida, segmented worm, Hirudinidae), Hubei, China	[33]
Aspernidine H (104)	457	C ₂₆ H ₃₅ NO ₆	<i>Whitmania pigra</i> (Annelida, segmented worm, Hirudinidae), Hubei, China	[33]
Emericellolide A (105)	559	C ₃₀ H ₄₁ NO ₉	<i>Tamarix chinensis</i> (Leaves, Tamaricaceae), Laizhou Bay, China	[39]
Emericellolide B (106)	559	C ₃₀ H ₄₁ NO ₉	<i>Tamarix chinensis</i> (Leaves, Tamaricaceae), Laizhou Bay, China	[39]
Emericellolide C (107)	545	C ₂₉ H ₃₉ NO ₉	<i>Tamarix chinensis</i> (Leaves, Tamaricaceae), Laizhou Bay, China	[39]
Emeriphenolicin E (108)	733	C ₄₄ H ₆₃ NO ₈	<i>Tamarix chinensis</i> (Leaves, Tamaricaceae), Laizhou Bay, China	[39]
Emeriphenolicin F (109)	733	C ₄₄ H ₆₃ NO ₈	<i>Tamarix chinensis</i> (Leaves, Tamaricaceae), Laizhou Bay, China	[39]
Emeriphenolicin G (110)	747	C ₄₅ H ₆₅ NO ₈	<i>Tamarix chinensis</i> (Leaves, Tamaricaceae), Laizhou Bay, China	[39]

* Mol. Wt.: Molecular weight; Mol. Formula: Molecular formula.

It was reported that biosynthesis of **99** starts with orsellinaldehyde from PKS-PkfA, which undergoes hydroxylation, one phenolic OH methylation, and prenylation to produce **197**. Subsequently, hydroxylation of **197** yields **198** [49]. It was hypothesized that **198** is oxidized to produce asperugin, and then it is transformed into aspernidine A (**99**) through a series of steps [49] (Scheme 4).

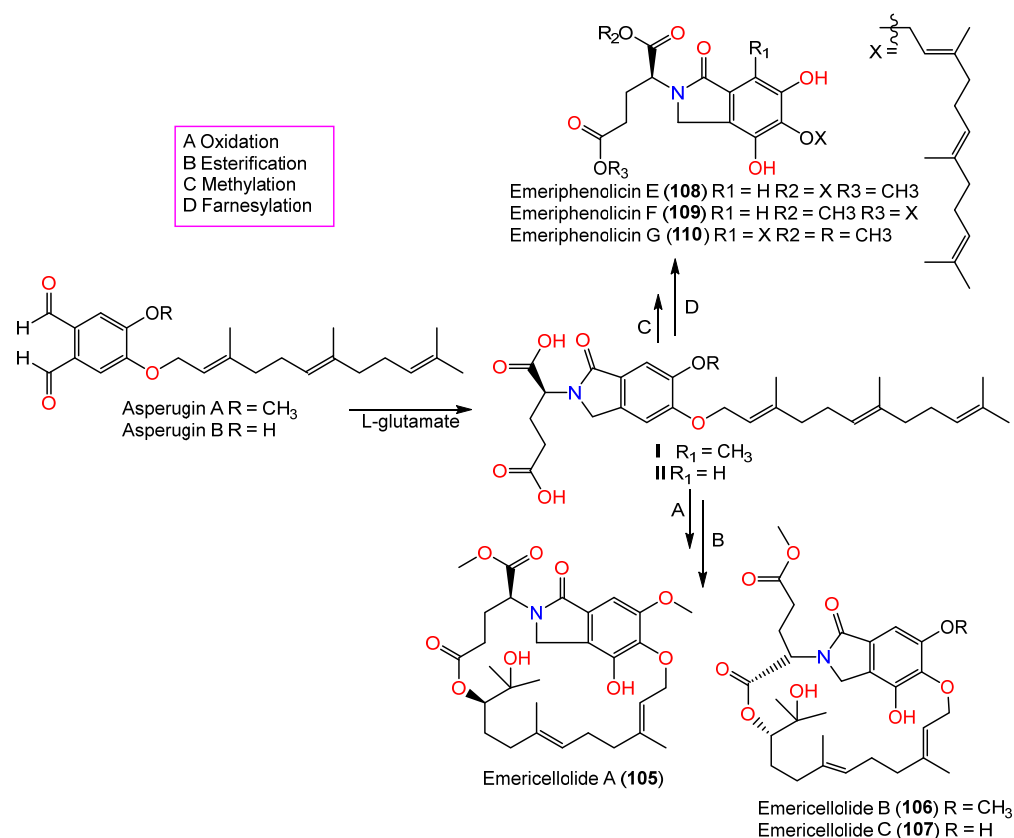


Scheme 4. Biosynthetic pathways of aspernidine A (99) [49].

From the red alga *Polysiphonia scopulorum* var. *villum*-associated *A. nidulans* EN-330, two new indole diterpenes are produced: 19-hydroxypenitrem A (93) and 19-hydroxypenitrem E (94), which are chlorinated and dechlorinated indole diterpenoids, respectively, along with known congeners 95 and 96, which were purified from the EtOAc cultures and acetone extracts by SiO₂/Sephadex LH-20/HPLC and characterized by NMR and CD analyses. These metabolites feature an indole skeleton produced from a tryptophan precursor (indole-3-glycerol-phosphate) and geranyl-geranyl diphosphate-derived cyclic diterpenoid framework. Penitrem A (95) belongs to a rare tremorgenic mycotoxins group that has a C-19 skeleton fused to C-2 and C-3 of the indole moiety. Compound 93 is like 95, but it has C19-oxygenated quaternary carbon instead of the methine in 95. Both 93 and 94 are 19S/22S/31R/32S configured. In the brine shrimp assay, 93–96 possessed potent cytotoxic effectiveness (LD₅₀s 3.2, 4.6, 1.7, and 8.7 µM, respectively), in comparison to colchicine (LD₅₀ 10.7 µM), where 93 and 95 were more powerful than 94, indicating that the C-6 Cl-substitution boosted the activity, while the 19-OH group suppressed it (93 vs. 95) [38]. In the assay for antibacterial activity against aquatic- (*E. tarda* and *V. anguillarum*) and human-pathogens (*E. coli* and *S. aureus*), 93–95 demonstrated moderate antimicrobial potential vs. *E. tarda*, *V. anguillarum*, *E. coli*, and *S. aureus* (MICs ranged from 16 to 64 µg/mL) [38].

From Annelida *Whitmania pigra*-associated *A. nidulans*, aspernidines F–H (102–104), new prenylated isoindolinone alkaloids were purified and characterized utilizing SiO₂/Sephadex LH-20/HPLC and spectral/ECD analyses, respectively. They possess a C5-linked C15 side chain. Compounds 103 and 104 exhibited moderate cytotoxic capacity on A-549, HL-60, SMMC-7721, SW-480, and MCF-7 (IC₅₀s ranged from 4.77 to 33.03 µM) compared to *cis*-platin (IC₅₀ 3.22–22.96 µM). It was observed that 104 exhibited powerful inhibitory capacity vs. SW-480 cells (IC₅₀s 4.77 µM) compared to *cis*-platin (IC₅₀s 18.01 µM) [33].

In 2016, novel meroterpenoids, emericellolides A–C (105–107) and emeriphenolicins E–G (108–110), with an isoindolone nucleus were separated from an *A. nidulans* HDN12.249 EtOAc broth extract isolated from *Tamarix chinensis* leaves that were obtained from Laizhou Bay using SiO₂/RP-18/Sephadex LH-20/HPLC. Compounds 105–107 are characterized by an unparalleled macrolide skeleton consisting of an isoindolone moiety, an uncommon L-glutamate unit, and a sesquiterpene unit, while emeriphenolicins E–G (108–110) are rare isoindolone-based meroterpenoids with two farnesyl units linked to the isoindolone unit. These metabolites were structurally elucidated using NMR, MS, Mo₂(AcO)₄-induced ECD, chemical conversion, and Marfey's method. In the SRB assay, only 108 exhibited selective potential vs. A549, HeLa, and HCT-116 (IC₅₀s 12.04, 4.77, and 33.05 µM, respectively); however, the others were ineffective (IC₅₀ > 50 µM) [39]. It was proposed that these metabolites were produced from asperugin A or B as an intermediate (Scheme 5). Further, farnesyl and L-glutamate units are formed through additional post-modifications, such as oxidation, methylation, and intra-molecular esterification [39].



Scheme 5. Biosynthesis pathways of 105–110 from asperugin A or B [39].

3.4.5. Other Nitrogenous Compounds

Compound **111** was purified from cultured *A. nidulans* MeOH extract using alumina CC and crystallization from water. This compound had cytotoxic capacity vs. KB cells (endpoint value of 10–25 µg/mL and lethal endpoint of 50–100 µg/mL) [67], as well as inhibition of HCV NS3/4A protease (IC₅₀ 24.5 µg/mL), compared with HCV-12 (IC₅₀ 1.5 µg/mL), in addition to its potent cytotoxicity with inhibition zone difference of 100–200 mm vs. L1210, CCRF-CEM, colon 38, H-125, and HEP-G2 in the disc diffusion assay [47] (Figure 10).

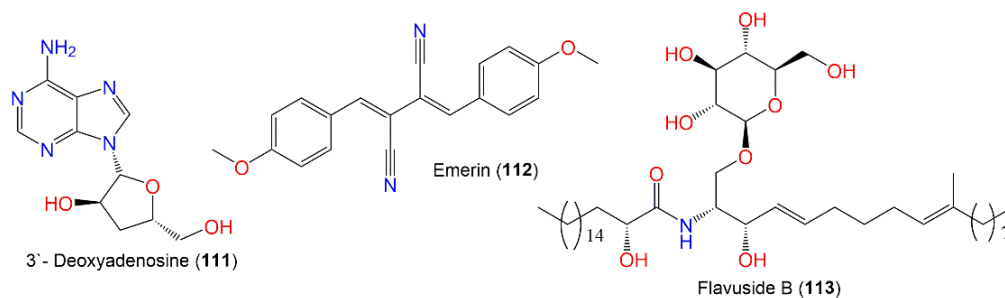


Figure 10. Structures of other nitrogenous compound (111–113) alkaloids.

The cerebroside, flavaside B (113), reported from orange peel-associated *E. nidulans*, had no antimalarial, antimicrobial, or antileishmanial capacities [68] (Table 8).

Table 8. Other nitrogenous compounds reported from *A. nidulans*.

Compound Name	Mol. Wt. *	Mol. Formula *	Host (Part, Family)/Location	Ref.
3'- Deoxyadenosine (111)	251	C ₁₀ H ₁₃ N ₅ O ₃	Cultured	[67]
	-	-	<i>Turbinaria elatensis</i> (Brown alga, <i>Phaeophyceae</i>), Egyptian Red Sea, Ras Mohamed, South Sina, Egypt	[47]
Emerin (112)	316	C ₂₀ H ₁₆ N ₂ O ₂	Cultured	[48]
Flavuside B (113)	755	C ₄₃ H ₈₁ N ₇ O ₉	Piece of orange peel (<i>Rutaceae</i>), Tifton, Georgia	[68]

* Mol. Wt.: Molecular weight; Mol. Formula: Molecular formula.

3.5. Peptides

Diverse strategies have evolved to take advantage of the biosynthetic stockpile of fungi. Various strategies are reported to better utilize the BGC (biosynthetic genes cluster) of this fungus.

The identification of aspercryptins (116–133), a new family of lipopeptides via prohibition of histone deacetylase (HDACi) in *A. nidulans*, was reported. They were discovered by NMR and MS/MS metabolite screening (Figures 11–14). These metabolites are six-amino-acid peptides, having two non-canonical α -amino acids derived from saturated C12 and C8 fatty acids and a C-terminal alcohol [69] (Table 9). Hence, HDACi could be utilized for finding out new metabolites, even from fungal species that were intensively investigated.

Table 9. Peptides reported from *A. nidulans*.

Compound Name	Mol. Wt.	Mol. Formula	Host (Part, Family)	Ref.
Nidulanin A (114)	603	C ₃₄ H ₄₅ N ₅ O ₅	Cultured	[56]
Echinocandin B (115)	1059	C ₅₂ H ₈₁ N ₇ O ₁₆	Cultured	[70]
Aspercryptin A1 (116)	757	C ₃₇ H ₇₁ N ₇ O ₉	Mutant strain cultured	[69]
Aspercryptin A2 (117)	741	C ₃₇ H ₇₁ N ₇ O ₈	Mutant strain cultured	[69]
<i>epi</i> -Aspercryptin A2 (118)	741	C ₃₇ H ₇₁ N ₇ O ₈	Mutant strain cultured	[69]
Aspercryptin A3 (119)	743	C ₃₆ H ₆₉ N ₇ O ₉	Mutant strain cultured	[69]
Aspercryptin A4 (120)	729	C ₃₅ H ₆₇ N ₇ O ₉	Mutant strain cultured	[69]
Aspercryptin A5 (121)	727	C ₃₆ H ₆₉ N ₇ O ₈	Mutant strain cultured	[69]
Aspercryptin A6 (122)	713	C ₃₅ H ₆₇ N ₇ O ₈	Mutant strain cultured	[69]
Aspercryptin A7 (123)	670	C ₃₄ H ₆₆ N ₆ O ₇	Mutant strain cultured	[69]
Aspercryptin B1 (124)	933	C ₄₇ H ₇₉ N ₇ O ₁₂	Mutant strain cultured	[69]
Aspercryptin B2 (125)	917	C ₄₇ H ₇₉ N ₇ O ₁₁	Mutant strain cultured	[69]
Aspercryptin B3 (126)	919	C ₄₆ H ₇₇ N ₇ O ₁₂	Mutant strain cultured	[69]
Aspercryptin B4 (127)	905	C ₄₅ H ₇₅ N ₇ O ₁₂	Mutant strain cultured	[69]
Aspercryptin C1 (128)	799	C ₃₉ H ₇₃ N ₇ O ₁₀	Mutant strain cultured	[69]
Aspercryptin C2 (129)	783	C ₃₉ H ₇₃ N ₇ O ₉	Mutant strain cultured	[69]
Aspercryptin C3 (130)	785	C ₃₈ H ₇₁ N ₇ O ₁₀	Mutant strain cultured	[69]
Aspercryptin C4 (131)	771	C ₃₇ H ₆₉ N ₇ O ₁₀	Mutant strain cultured	[69]
Aspercryptin C6 (132)	755	C ₃₇ H ₆₉ N ₇ O ₉	Mutant strain cultured	[69]
Aspercryptin D1 (133)	813	C ₄₀ H ₇₅ N ₇ O ₁₀	Mutant strain cultured	[69]

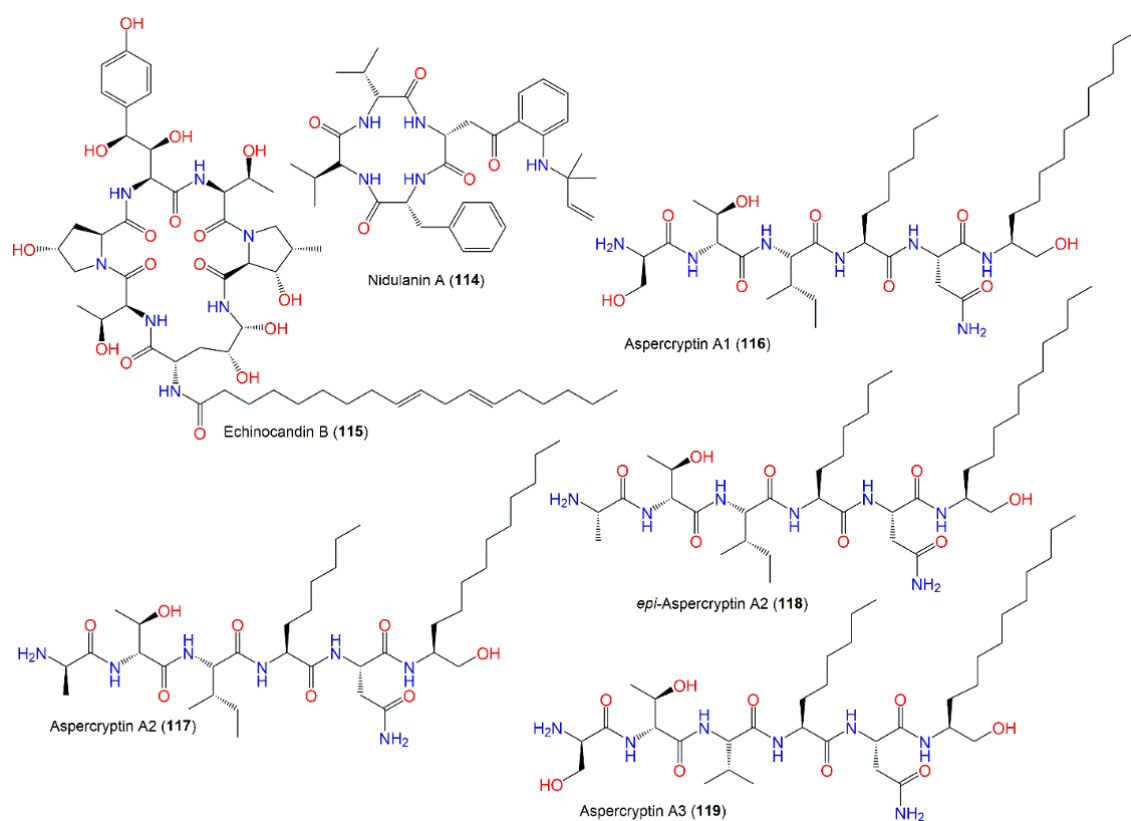


Figure 11. Structures of peptides (114–119).

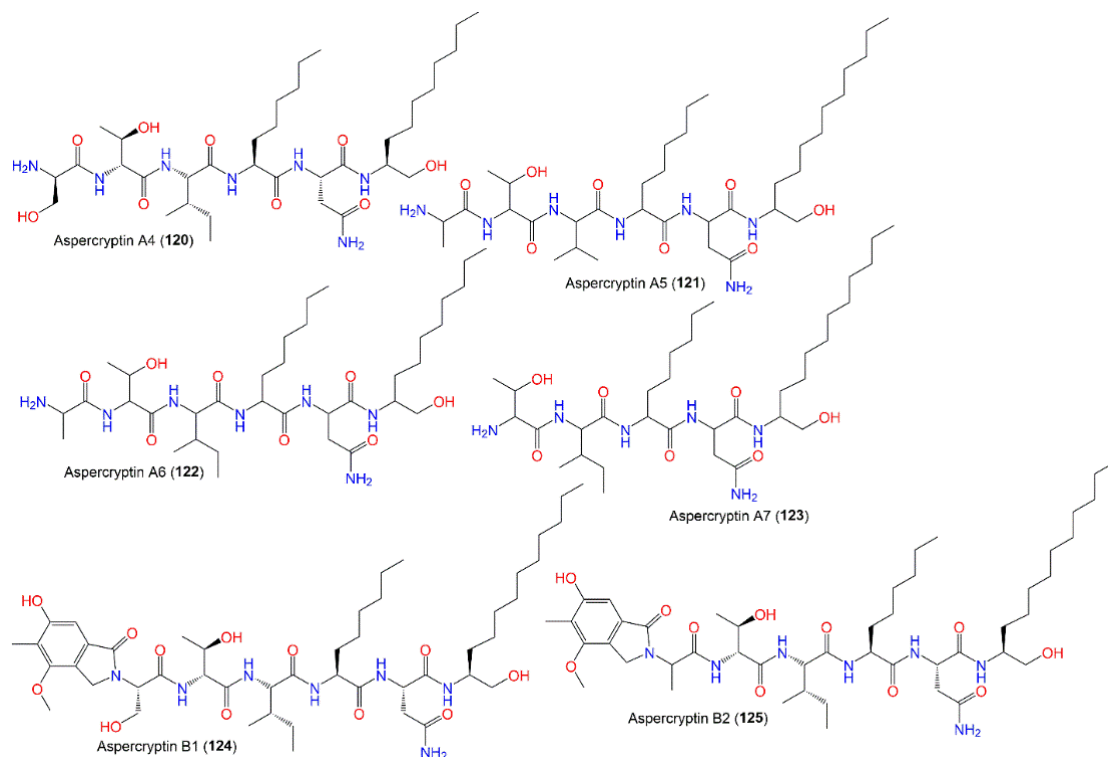


Figure 12. Structures of peptides (120–125).

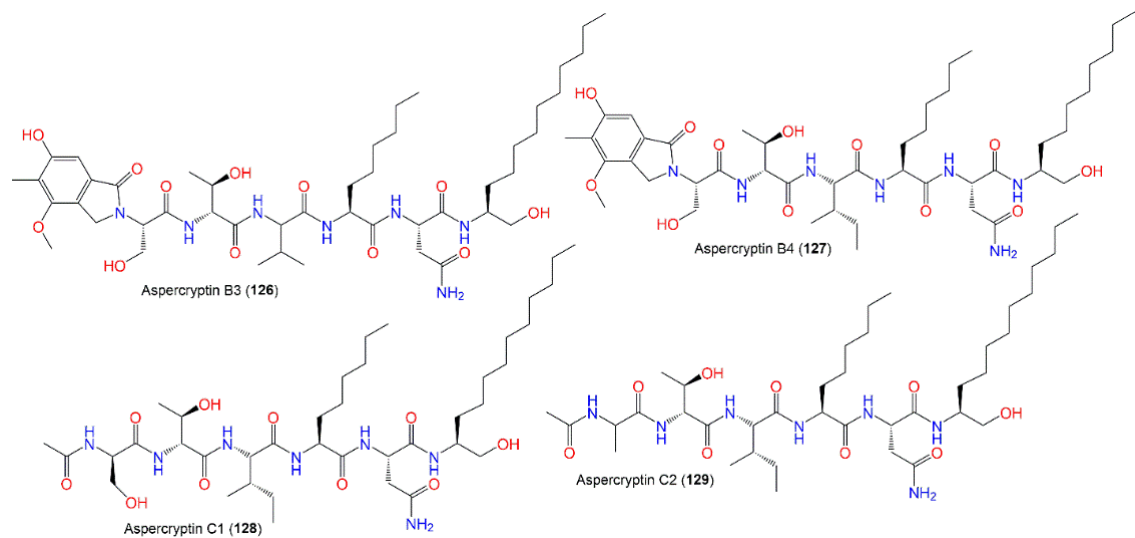


Figure 13. Structures of peptides (126–129).

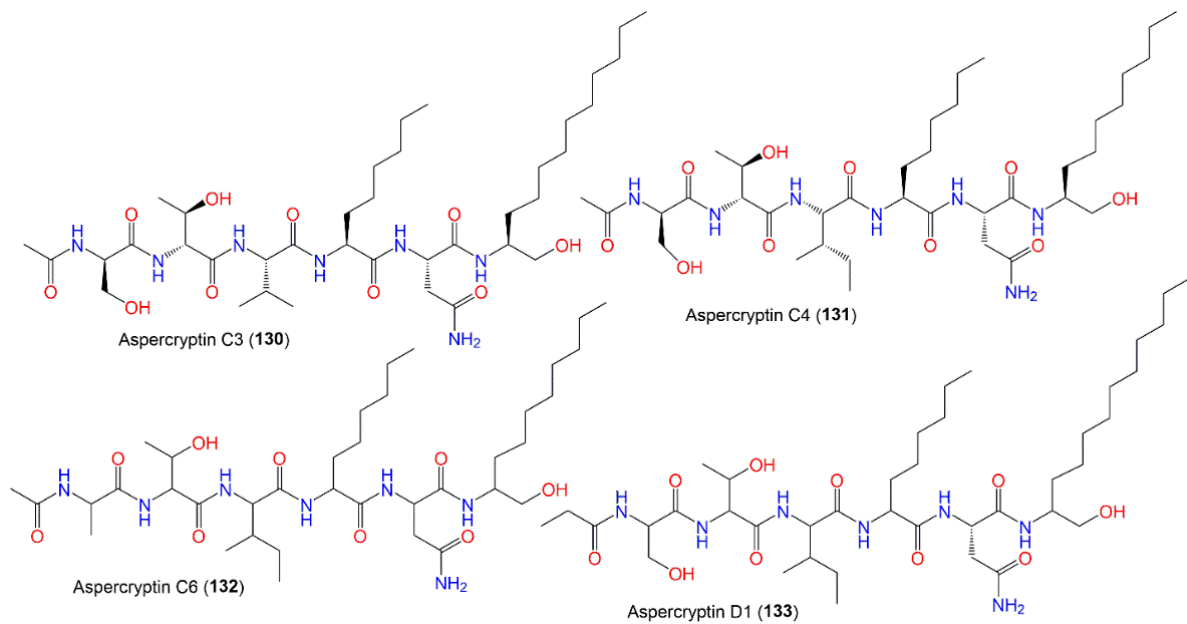


Figure 14. Structures of peptides (130–133).

3.6. Terpenoids and Sterols

Terpenoids and sterols are among the metabolites reported from *E. nidulans* that are derived from mevalonate via a key step of cyclization and elimination reaction, respectively.

The engineered *A. nidulans* biosynthesized **134**, which was extracted using ASE (accelerated solvent extraction) and purified by HPLC (Table 10). In the DPPH assays, it had more powerful antioxidant potential than beta-carotene; however, it had no antimicrobial or anti-*Leishmanial* (50 μ M) potential [71].

Table 10. Terpenes reported from *A. nidulans*.

Compound Name	Mol. Wt.	Mol. Formula	Host (Part, Family)/Location	Ref.
<i>ent</i> -Pimara-8(14),15-diene (134)	272	C ₂₀ H ₃₂	Engineered cultured	[71]
Neoaustrinone (135)	442	C ₂₅ H ₃₀ O ₇	Cultured	[56]
Niduterpenoid A (136)	404	C ₂₅ H ₄₀ O ₄	<i>Whitmania pigra</i> Whitman (Annelida, segmented worm, <i>Hirudinidae</i>), Hubei, China	[40]
Niduterpenoid B (137)	404	C ₂₅ H ₄₀ O ₄	<i>Whitmania pigra</i> Whitman (Annelida, segmented worm, <i>Hirudinidae</i>), Hubei, China	[40]
Austin (138)	500	C ₂₇ H ₃₂ O ₉	Cultured	[72]
Dehydroaustin (139)	498	C ₂₇ H ₃₀ O ₉	Cultured	[72]
Acetoxydehydroaustin (140)	556	C ₂₉ H ₃₂ O ₁₁	Cultured	[72]
Austinolide (141)	442	C ₂₅ H ₃₀ O ₇	Cultured	[56]
Austinol (142)	458 -	C ₂₅ H ₃₀ O ₈ -	Cultured Deep-sea sediment, South China Sea	[44,49,72] [31]
Dehydroaustinol (143)	456 -	C ₂₅ H ₂₈ O ₈ -	Cultured Deep-sea sediment, South China Sea	[44,49,72] [31]
β-Amyrin (144)	426	C ₃₀ H ₅₀ O	Cultured	[73]

In 1983, β-amyrin was the first triterpenoid separated from *A. nidulans* [73]. From *Whitmania pigra* (Annelida, segmented worm)-associated *A. nidulans*, new sesterterpenoids, niduterpenoids A (**136**) and B (**137**), were reported that were purified from the EtOH culture extract by SiO₂/Sephadex LH-20/HPLC (Figure 15). These metabolites were distinguished by a highly congested 5/5/5/5/3/5 hexacyclic skeleton without unsaturated functional groups, based on spectral and X-ray analyses [40]. They were assessed for their ERα (estrogen receptor α) inhibitory and cytotoxic potential vs. MCF-7 in the MTT assay. Compound **136** had no obvious cytotoxic potential, even at 80 μM, while it abolished the 17-estradiol-induced cell proliferation (IC₅₀ 11.42 μM) in a dose-based way. Molecular docking revealed that **136** and **137** fitted well with the ERα ligand-binding site and partially occupied the lasofoxifene (potent Er modulator) whole pocket. They formed key H-bonds with Arg346/Glu353/Met295 and a highly hydrophobic envelope with Leu298/Phe356/Phe377/Met294/Leu354. These findings indicated **136** was a potential ERα antagonist that required further studies [40].

These metabolites are the first reported sesterterpenes with a hexacyclic ring system having an uncommon cyclopropane moiety (Scheme 6). It was proposed that they were biosynthesized from GFPP through various cyclization and Wagner–Meerwein alkyl shift and hydride reactions, producing the **X** (key intermediate) with a hexacyclic 5/5/5/5/3/5 framework. Additional oxidation reactions result in **136** and **137** [40].

Compounds **138**, **139**, and **142** are meroterpenoids separated from a cold spring, deep-sea-sediment-associated strain that had no antimicrobial capacity vs. aquatic/human bacteria and pathogenic plant fungi [31].

The separation of new metabolites **145** and **148–150** was reported, in addition to **146**, **151–154**, and **156** from the EtOAc extract of the fungus *A. nidulans*, utilizing SiO₂/Sephadex LH-20/HPLC and elucidated by spectral, ECD, and X-ray analyses (Figure 16).

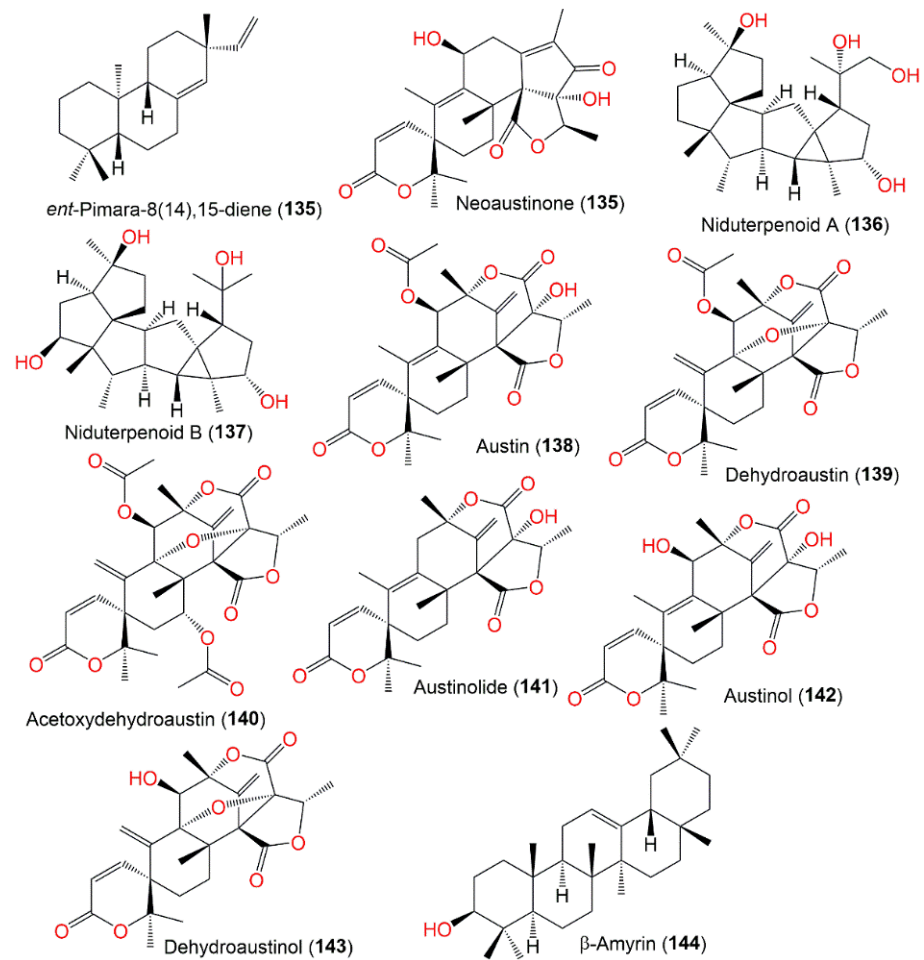
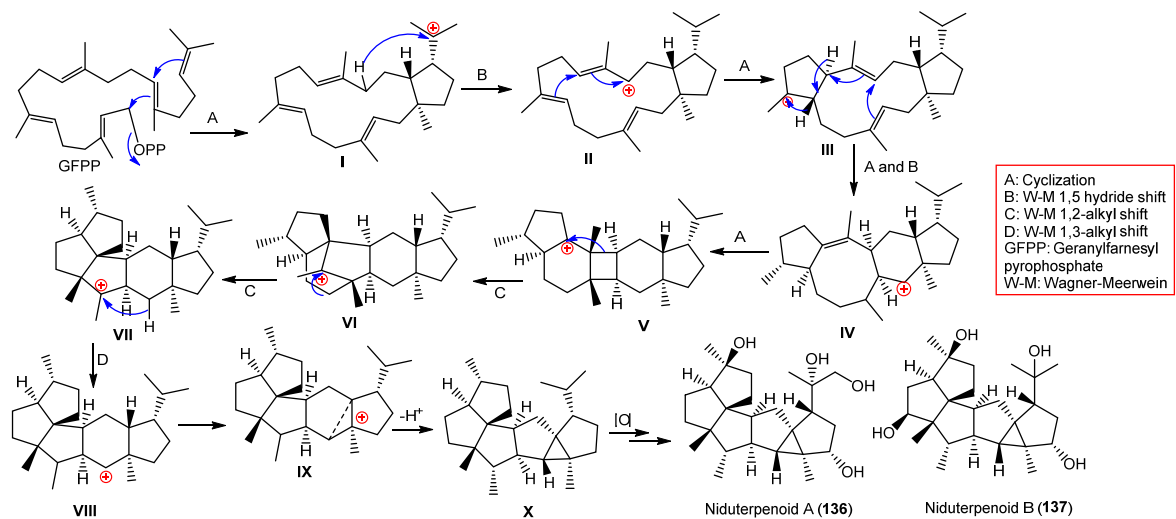


Figure 15. Structures of terpenoids (135–144).



Scheme 6. Biosynthesis of niduterpenoids A (136) and B (137) from GFPP [40].

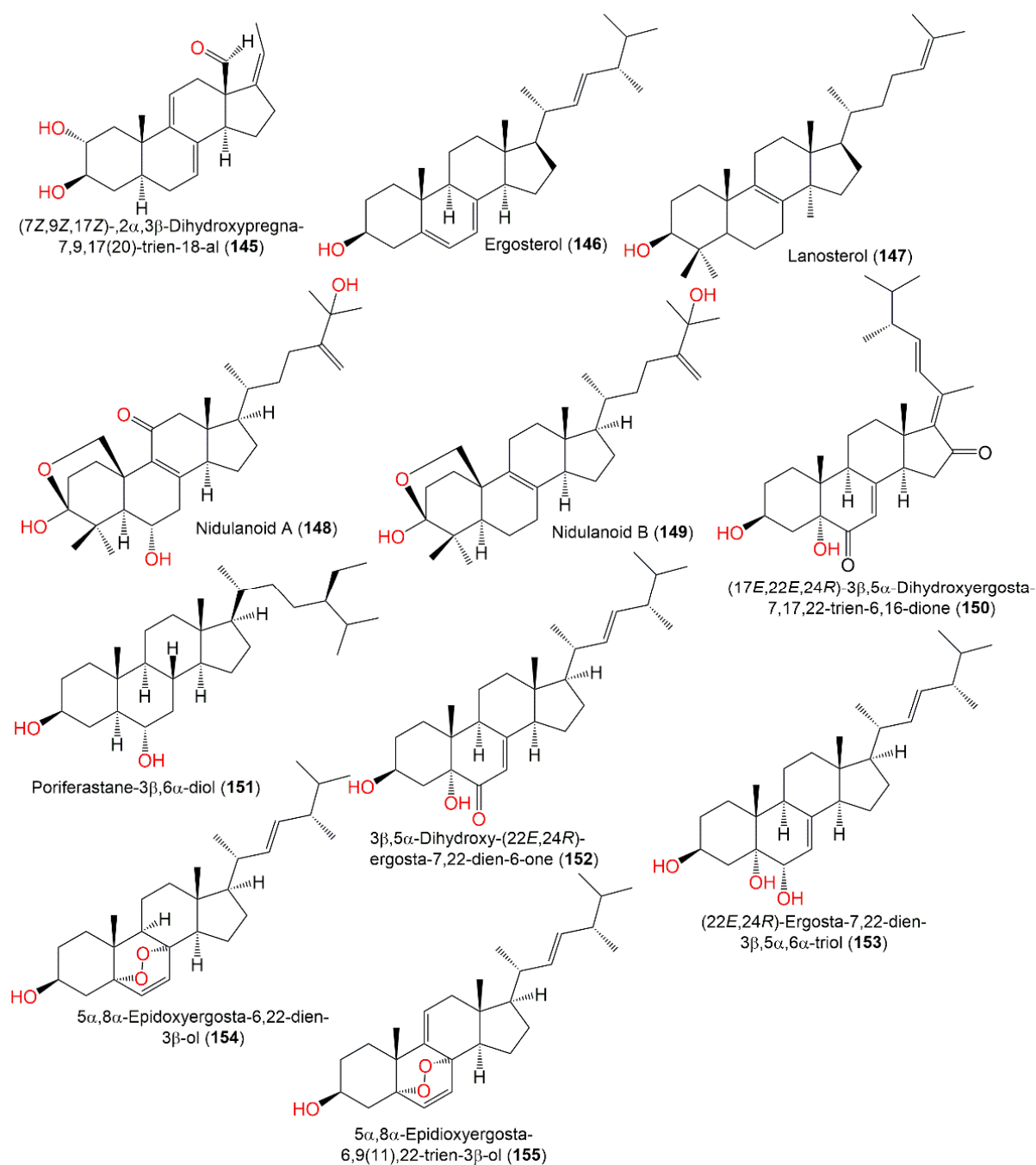


Figure 16. Structures of sterols (**145–155**).

These metabolites were assessed for cytotoxic potential in vitro vs. the PC12 cell line in the MTT assay. Only **145** possessed moderate potential (IC_{50} 7.34 μ M) compared to doxorubicin (IC_{50} 5.71 μ M) [41]. Compound **167**, reported from the EtOAc broth extract of *Emericella nidulans*, was mildly active as an HCV inhibitor (IC_{50} 47.0 μ g/mL) relative to HCV-12 (IC_{50} 1.5 μ g/mL) [47] (Figure 17, Table 11).

Table 11. Sterols reported from *A. nidulans*.

Compound Name	Mol. Wt.	Mol. Formula	Host (Part, Family)/Location	Ref.
(7Z,9Z,17Z)-,2 α ,3 β -Dihydroxypregna-7,9,17(20)-trien-18-al (145)	328	C ₂₁ H ₂₈ O ₃	<i>Whitmania pigra</i> (Annelida, segmented worm, <i>Hirudinidae</i>), Qichun city, Hubei, China	[41]
Ergosterol (146)	396	C ₂₈ H ₄₄ O	Cultured	[41,74]
	-	-	Deep-sea sediment of the western Pacific Ocean, China	[58]
	-	-	<i>Nyctanthes arbor-tristis</i> (<i>Oleaceae</i>), Sabira	[53]
	-	-	Piece of orange peel (<i>Rutaceae</i>), Tifton, Georgia	[68]
Lanosterol (147)	426	C ₃₀ H ₅₀ O	Cultured	[74]
Nidulanoid A (148)	486	C ₃₀ H ₄₆ O ₅	<i>Whitmania pigra</i> (Annelida, segmented worm, <i>Hirudinidae</i>), Qichun city, Hubei, China	[41]
Nidulanoid B (149)	456	C ₃₀ H ₄₈ O ₃	<i>Whitmania pigra</i> (Annelida, segmented worm, <i>Hirudinidae</i>), Qichun city, Hubei, China	[41]
(17E,22E,24R)-3 β ,5 α -Dihydroxyergosta-7,17,22-trien-6,16-dione (150)	440	C ₂₈ H ₄₀ O ₄	<i>Whitmania pigra</i> (Annelida, segmented worm, <i>Hirudinidae</i>), Qichun city, Hubei, China	[41]
Poriferastane-3 β ,6 α -diol (151)	432	C ₂₉ H ₅₂ O ₂	<i>Whitmania pigra</i> (Annelida, segmented worm, <i>Hirudinidae</i>), Qichun city, Hubei, China	[41]
3 β ,5 α -Dihydroxy-(22E,24R)-ergosta-7,22-dien-6-one (152)	428	C ₂₈ H ₄₄ O ₃	<i>Whitmania pigra</i> (Annelida, segmented worm, <i>Hirudinidae</i>), Qichun city, Hubei, China	[41]
(22E,24R)-Ergosta-7,22-dien-3 β ,5 α ,6 α -triol (153)	430	C ₂₈ H ₄₆ O ₃	<i>Whitmania pigra</i> (Annelida, segmented worm, <i>Hirudinidae</i>), Qichun city, Hubei, China	[41]
5 α ,8 α -Epidoxyergosta-6,22-dien-3 β -ol (154)	428	C ₂₈ H ₄₄ O ₃	<i>Whitmania pigra</i> (Annelida, segmented worm, <i>Hirudinidae</i>), Qichun city, Hubei, China	[41]
	-	-	Deep-sea sediment, western Pacific Ocean, China	[58]
5 α ,8 α -Epidoxyergosta-6,9(11),22-trien-3 β -ol (155)	426	C ₂₈ H ₄₂ O ₃	Deep-sea sediment, western Pacific Ocean, China	[58]
	-	-	<i>Turbinaria elatensis</i> (Brown alga, <i>Phaeophyceae</i>), Egyptian Red Sea, Ras Mohamed, South Sina, Egypt	[47]
(22E)-3 β ,4 β ,5 α -Trihydroxyergosta-7,22-dien-6-one (156)	444	C ₂₈ H ₄₄ O ₄	<i>Whitmania pigra</i> (Annelida, segmented worm, <i>Hirudinidae</i>), Qichun city, Hubei, China	[41]
5 α ,6 α -Epoxy-3 β -hydroxy-(22E)-ergosta-8(14),22-dien-7-one (157)	426	C ₂₈ H ₄₂ O ₃	Deep-sea sediment, western Pacific Ocean, China	[58]
3 β ,5 α ,9 α -Trihydroxyergosta-7,22-diene-6-one (158)	444	C ₂₈ H ₄₄ O ₄	Deep-sea sediment, western Pacific Ocean, China	[58]
3 β ,5 α -Dihydroxy-6 β -acetox-ergosta-7,22-diene (159)	458	C ₃₀ H ₅₀ O ₃	Deep-sea sediment, western Pacific Ocean, China	[58]
3 β ,5 α ,6 β ,22E-Ergosta-7,22-diene-3,5,6-triol 6-palmitate (160)	668	C ₄₄ H ₇₆ O ₄	Deep-sea sediment, western Pacific Ocean, China	[58]

Table 11. Cont.

Compound Name	Mol. Wt.	Mol. Formula	Host (Part, Family)/Location	Ref.
Nuatigenin (161)	430	C ₂₇ H ₄₂ O ₄	Deep-sea sediment, western Pacific Ocean, China	[58]
1-Dehydronuatigenone (162)	426	C ₂₇ H ₃₈ O ₄	Deep-sea sediment, western Pacific Ocean, China	[58]
1-Dehydroisnuatigenone (163)	426	C ₂₇ H ₃₈ O ₄	Deep-sea sediment, western Pacific Ocean, China	[58]
3 β ,15 α -Dihydroxyl-(22 <i>E</i> ,24 <i>R</i>)-ergosta-5,8(14),22-trien-7-one (164)	426	C ₂₈ H ₄₂ O ₃	Deep-sea sediment, western Pacific Ocean, China	[58]
3 β ,15 β -Dihydroxyl-(22 <i>E</i> ,24 <i>R</i>)-ergosta-5,8(14),22-trien-7-one (165)	426	C ₂₈ H ₄₂ O ₃	Deep-sea sediment, western Pacific Ocean, China	[58]
β -Sitosterol-3-O- β -D-glucoside (166)	576	C ₃₅ H ₆₀ O ₆	Piece of orange peel (Rutaceae), Tifton, Georgia	[68]
Ergosterol peroxide (167)	428	C ₂₈ H ₄₄ O ₃	<i>Turbinaria elatensis</i> (Brown alga, <i>Phaeophyceae</i>), Egyptian Red Sea, Ras Mohamed, South Sina, Egypt	[47]

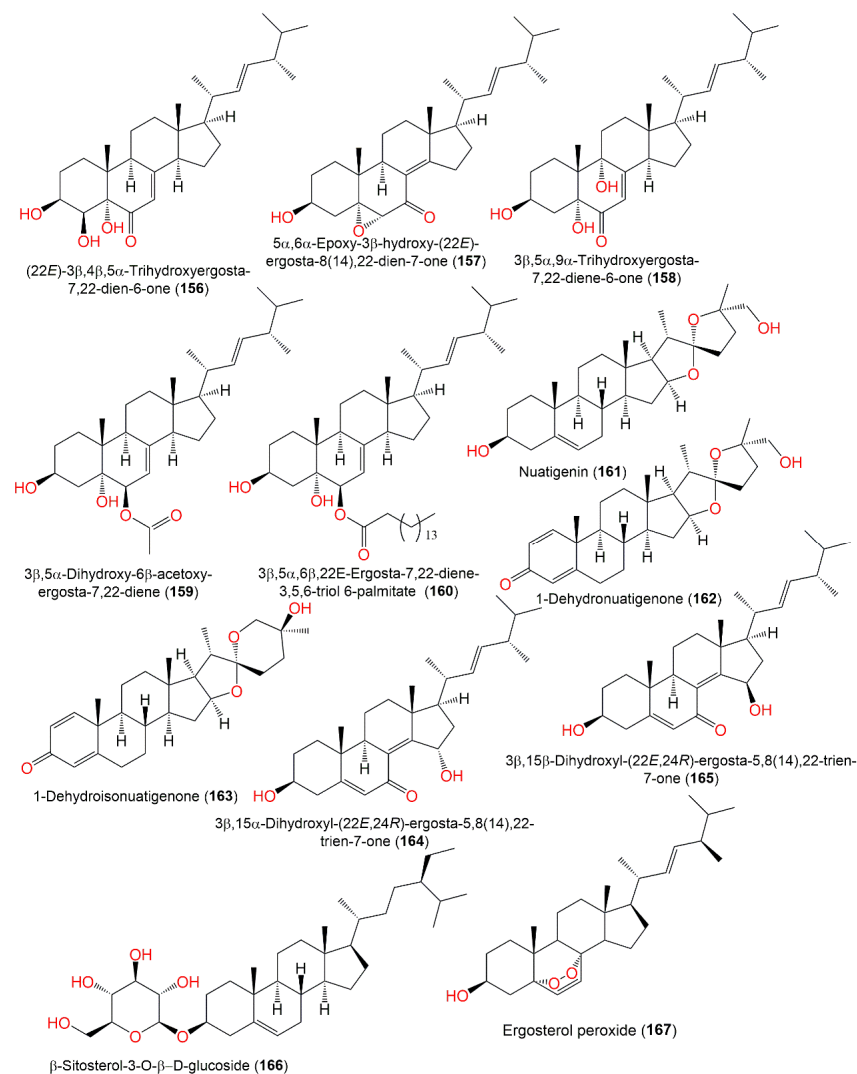


Figure 17. Structures of sterols (156–167).

3.7. Lactones and Furanones

A new metabolite, **172**, was separated from the acetone culture extract of *A. nidulans* IFO6398 by SiO₂ CC using benzene as eluent. It featured two mono-substituted phenyl and maleic anhydride moieties; this compound was assigned by spectral analyses. In the radish seedlings bioassay, **172** accelerated root elongation (Conc. 30 and 100 g/L, respectively), while it had no notable influence on the hypocotyl elongation at the same concentrations. Moreover, **172** boosted root elongation and prohibited hypocotyl growth (Conc. 100 mg/L) in the lettuce seedling bioassay [75]. Compound **179**, separated from the *A. nidulans* IFO6398 acetone extract, boosted root elongation (Conc. 30 g/L) and showed no notable effect on lettuce seedling growth (Conc. 3, 10, 30, and 100 mg/L) in the radish and lettuce seedling bioassays, respectively [75] (Table 12).

Table 12. Furan and pyran derivatives reported from *A. nidulans*.

Compound Name	Mol. Wt.	Mol. Formula	Host (Part, Family)	Ref.
Nidulol (168)	194	C ₁₀ H ₁₀ O ₄	Cultured	[51]
Porriolide (169)	194	C ₁₀ H ₁₀ O ₄	Cultured	[57]
3-Methoxyporriolide (170)	224	C ₁₁ H ₁₂ O ₅	Cultured	[57]
7-Methoxyporriolide (171)	224	C ₁₁ H ₁₂ O ₅	Cultured	[57]
3-Carboxy-2,4-diphenyl-but-2-enoic anhydride (172)	264	C ₁₇ H ₁₂ O ₃	Cultured	[75]
Microperfuranone (173)	266	C ₁₇ H ₁₄ O ₃	Green alga, Sardinia, Italy, Mediterranean Sea	[43]
	-	-	Soil, Hell Valley, Noboribetsu, Hokkaido, Japan	[52]
	-	-	Cultured	[57]
	-	-	Deep-sea sediment, South China Sea	[31]
9-Hydroxymicroperfuranone (174)	282	C ₁₇ H ₁₄ O ₄	Soil, Hell Valley, Noboribetsu, Hokkaido, Japan	[52]
	-	-	Deep-sea sediment, South China Sea	[31]
Helvafuranone (175)	298	C ₁₇ H ₁₄ O ₅	Soil, Hell Valley, Noboribetsu, Hokkaido, Japan	[52]
Asperfuranone (176)	332	C ₁₉ H ₂₄ O ₅	Mutant strain cultured	[76]
Cichorine intermediate (177)	196	C ₁₀ H ₁₂ O ₄	Cultured	[56]
(4 <i>S</i> ,5 <i>R</i>)-4-Hydroxy-5-methylfuran-2-one (178)	132	C ₅ H ₈ O ₄	Piece of orange peel (<i>Rutaceae</i>), Tifton, Georgia	[68]
Asperlin (U-13,933) (179)	212	C ₁₀ H ₁₂ O ₅	Cultured	[75,77,78]
Chloro-asperlin (180)	248	C ₁₀ H ₁₃ ClO ₅	Cultured	[77]
Versiol (181)	262	C ₁₆ H ₂₂ O ₃	Deep-sea sediment, western Pacific Ocean, China	[58]
PsiAα (182)	294	C ₁₈ H ₃₀ O ₃	Cultured	[79]
PsiAβ (183)	296	C ₁₈ H ₃₂ O ₃	Cultured	[79]
Trichodermatide B (184)	264	C ₁₆ H ₂₄ O ₃	Piece of orange peel (<i>Rutaceae</i>), Tifton, Georgia	[68]
Koninginin A (185)	284	C ₁₆ H ₂₈ O ₄	Piece of orange peel (<i>Rutaceae</i>), Tifton, Georgia	[68]
Koninginin E (186)	282	C ₁₆ H ₂₆ O ₄	Piece of orange peel (<i>Rutaceae</i>), Tifton, Georgia	[68]
Koninginin H (187)	298	C ₁₆ H ₂₆ O ₅	Piece of orange peel (<i>Rutaceae</i>), Tifton, Georgia	[68]
Asperlinol (188)	230	C ₁₀ H ₁₄ O ₆	Cultured	[77]

Microperfurane (173), purified and characterized from *E. nidulans* var. *acristata*, had no antimicrobial, cytotoxic, and immune-stimulating activity [43], while 173 and 174 had antimicrobial potential against aquatic, human, and plant pathogens (MICs ranged from 4 to 64 $\mu\text{g/mL}$), whereas 173 presented notable effectiveness vs. *E. ictarda* (MIC 4 $\mu\text{g/mL}$) compared to chloramphenicol (MIC 2 $\mu\text{g/mL}$) [31] (Figure 18).

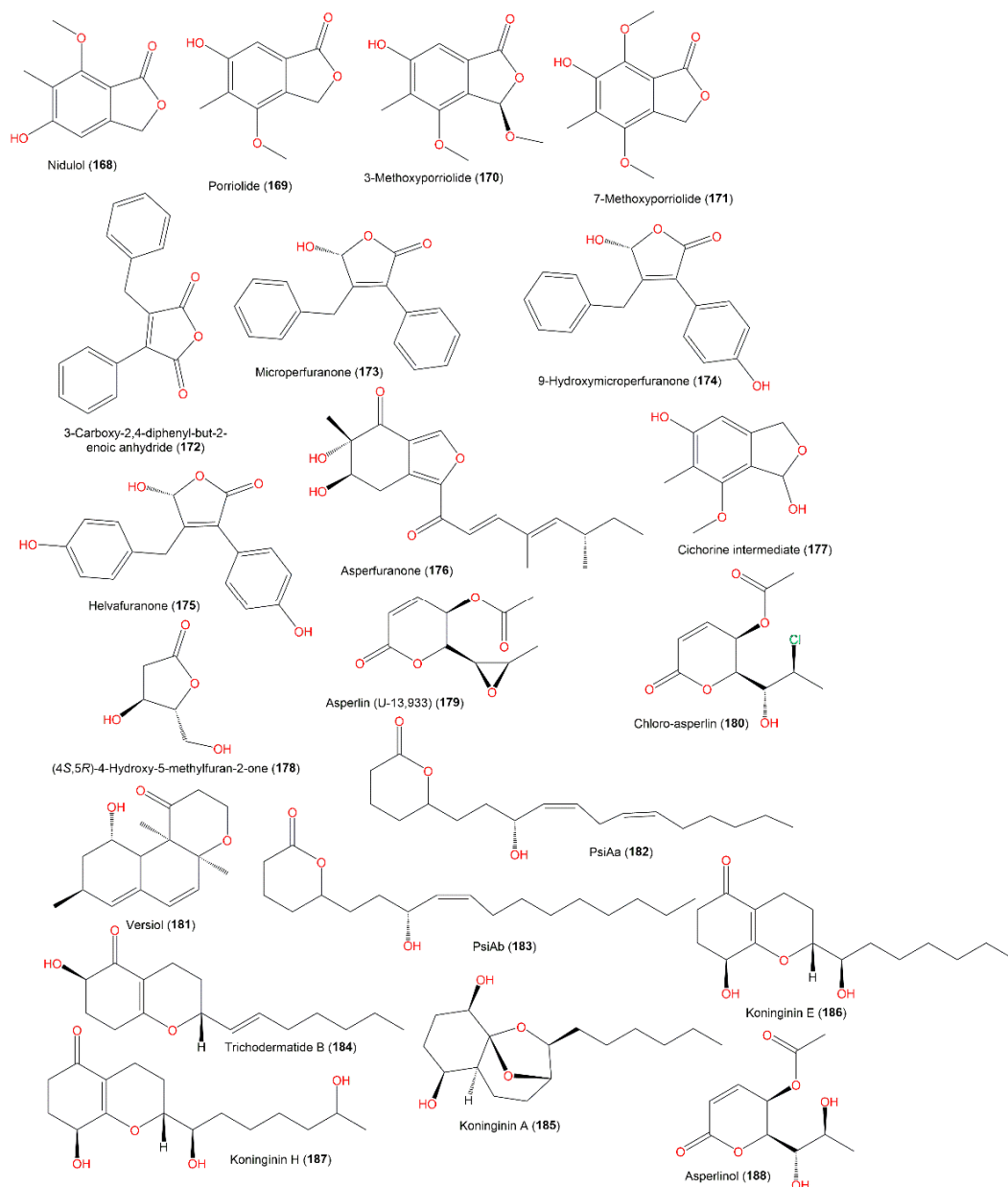


Figure 18. Structures of furan (168–178) and pyran (179–188) derivatives.

3.8. Polyketides and Glycerides

A new polyketide, koniginin H (187), together with 184–186 and 193–196, was reported from *E. nidulans* isolated from an orange peel (Figure 19, Table 13). Compound 187 belongs to the koniginin class of metabolites that was encountered in the *Trichoderma* genus [68]. An antimicrobial assessment of these metabolites vs. a panel of micro-organisms revealed that only 184 had good antifungal potential vs. *C. neoformans* (IC₅₀ 4.9 $\mu\text{g/mL}$) [68].

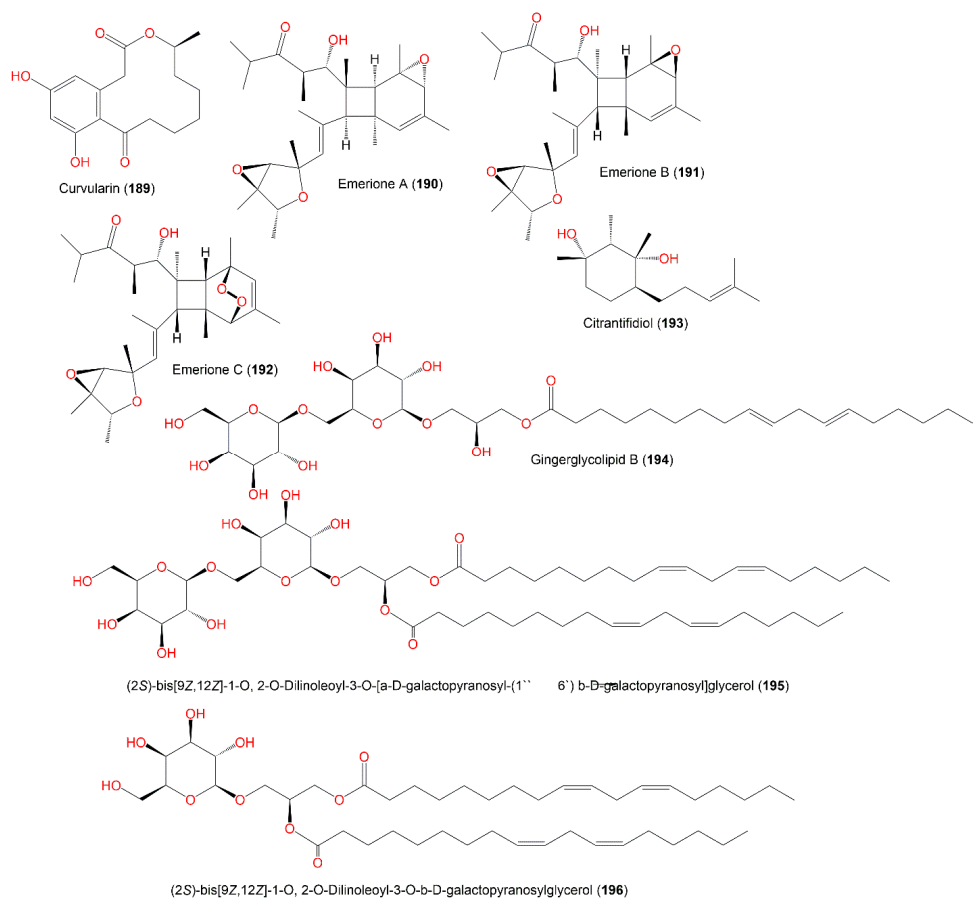
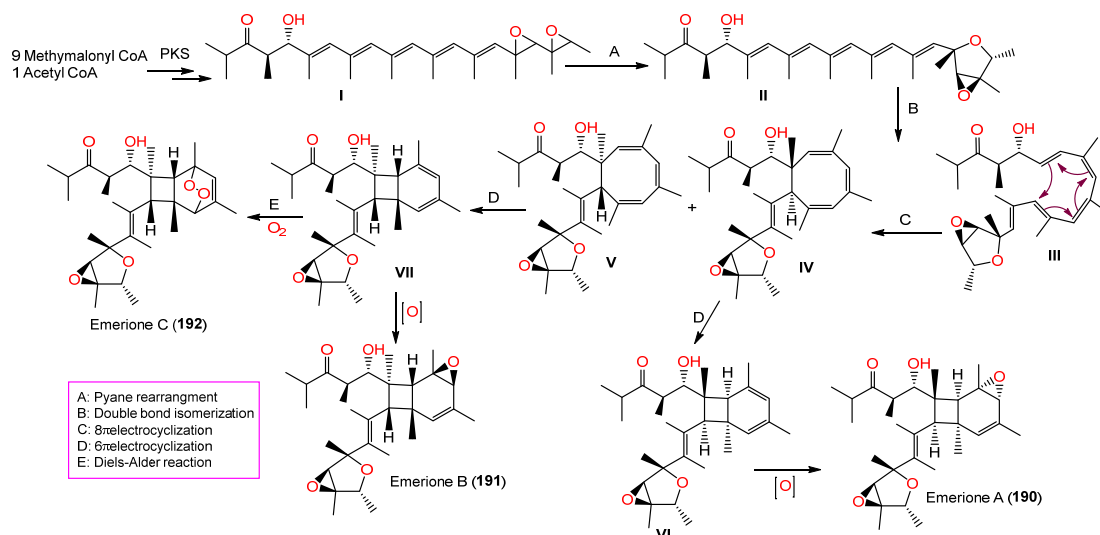


Figure 19. Structures of polyketides (189–193) and glycerides (194–196).

Table 13. Polyketides and glycerides reported from *A. nidulans*.

Compound Name/Chemical Class	Mol. Wt.	Mol. Formula	Host (Part, Family)	Ref.
Polyketides				
Curvularin (189)	292	C ₁₆ H ₂₀ O ₅	Deep-sea sediment, South China Sea	[31]
Emerione A (190)	472	C ₂₉ H ₄₄ O ₅	<i>Whitmania pigra</i> (Annelida, segmented worm, <i>Hirudinidae</i>), Hubei, China	[80]
Emerione B (191)	472	C ₂₉ H ₄₄ O ₅	<i>Whitmania pigra</i> (Annelida, segmented worm, <i>Hirudinidae</i>), Hubei, China	[80]
Emerione C (192)	488	C ₂₉ H ₄₄ O ₆	<i>Whitmania pigra</i> (Annelida, segmented worm, <i>Hirudinidae</i>), Hubei, China	[80]
Citrantifidiol (193)	240	C ₁₅ H ₂₈ O ₂	Piece of orange peel (<i>Rutaceae</i>), Tifton, Georgia	[68]
Glycerides				
Glycerglycolipid B (194)	678	C ₃₃ H ₅₈ O ₁₄	Piece of orange peel (<i>Rutaceae</i>), Tifton, Georgia	[68]
(2S)-bis[9Z,12Z]-1-O, 2-O-Dilinoleoyl-3-O-[α-D-galactopyranosyl-(1''→6') β-D-galactopyranosyl]glycerol (195)	940	C ₅₁ H ₈₈ O ₁₅	Piece of orange peel (<i>Rutaceae</i>), Tifton, Georgia	[68]
(2S)-bis[9Z,12Z]-1-O, 2-O-dilinoleoyl-3-O-β-D-galactopyranosylglycerol (196)	778	C ₄₅ H ₇₈ O ₁₀	Piece of orange peel (<i>Rutaceae</i>), Tifton, Georgia	[68]

New metabolites, emeriones A–C (**190–192**), were purified from an EtOH extract of the culture broth of endophytic *E. nidulans*, obtained from *Whitmania pigra* by SiO₂/Sephadex LH-20/HPLC. These metabolites are high-methylated polyketides with 3,6-dioxabicyclo[3.1.0]hexane and bicyclo[4.2.0]octene functionalities and were characterized using spectroscopic, X-ray, and CD analyses as well as ECD calculations. Compounds **190** and **191** are similar but differ in their configuration at the C9, C12, and C13 epoxy rings, possessing 2R/3R/4S/5S/8R/9S/12R/13S/14S/15S/16S/17R and 2R/3R/4S/5S/8S/9R/12S/13R/14R/15R/16S/17R configurations, respectively. Moreover, **192** has an extra peroxide bridge that results in an unusual 7,8-dioxatricyclo[4.2.2.0^{2,5}]decene scaffold construction. The NO production inhibitory efficacy of **190** and **191** was tested on LPS-mediated NO production in RAW264.7 using a CCK-8 assay. Interestingly, **190** demonstrated inhibition potential vs. NO production with a percent inhibition of NO production of 68.3% at a concentration of 10.0 µM, compared to indomethacin (with a percent inhibition of NO production of 84.2%, Conc. 40 µM); however, **191** had no effectiveness, although it possesses the same structure as **190** and differs only in the bicyclo[4.2.0]octane core absolute configuration [80]. They were assumed to be synthesized from methylmalonyl CoA (9 molecules) and acetyl-CoA (one molecule) by polyketide synthase to produce **I** (Scheme 7), which generates **II** via a Payne rearrangement that features a 3,6-dioxabicyclo[3.1.0]hexane moiety (Scheme 7).



Scheme 7. Biosynthesis of emeriones A–C (**190–192**) [81].

An octatonic ring is then formed through 8 π electrocyclization and double bond isomerization to produce **IV** and **V**, which undergo 6 π electrocyclizations to yield **VI** and **VII**, with a pair of mirror-image bicyclo[4.2.0]-octene frameworks. Further, **190** and **191** are created through an additional C-12 double bond epoxidation, while **192** is formed through a Diels–Alder reaction between an O₂ molecule and a bicyclo[4.2.0]octene core (Scheme 7) [80].

3.9. Other Metabolites

Asperbenzaldehyde (**199**) with an aromatic ring represents a new class of metabolites with tau aggregation inhibition potential. Moreover, its modified derivatives displayed noticeable lipoxygenase inhibition, suggesting its derived metabolites could exhibit dual activity [54].

The mycelia acetone extract of mutant *A. nidulans* LO2955 cultured on liquid lactose produced **202** (amount \approx 200 mg/L), which was not found in such amounts in the wild strain culture. This compound had lipoxygenase-1 inhibition (IC₅₀ 97.2 µM) [42].

Asperoxide A (**206**), a new acyclic peroxide analog, and **203** were biosynthesized by *A. nidulans* SD531 obtained from cold spring, deep-sea sediment in the South China Sea by

SiO₂/RP-18 CC and characterized by NMR and MS analyses [31] (Figure 20, Table 14). Their antimicrobial potential was examined vs. various aquatic/human bacteria and pathogenic plant fungi using a serial dilution technique. Compound 206 demonstrated antimicrobial effectiveness vs. *V. harveyi*, *A. hydrophilia*, *V. parahaemolyticus*, and *E. tarda* (MICs ranged from 16 to 64 µg/mL) [31].

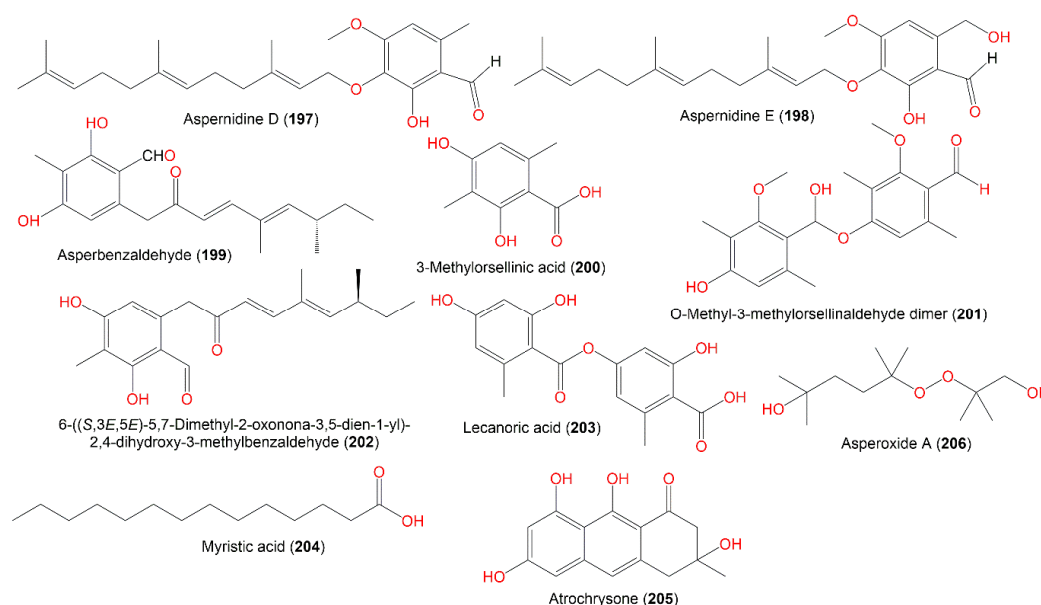


Figure 20. Structures of other metabolites (197–206).

Table 14. Other metabolites reported from *A. nidulans*.

Compound Name	Mol. Wt.	Mol. Formula	Host (Part, Family)	Ref.
Aspernidine D (197)	386	C ₂₄ H ₃₄ O ₄	Cultured	[49]
Aspernidine E (198)	402	C ₂₄ H ₃₄ O ₅	Cultured	[49]
Asperbenzaldehyde (199)	316	C ₁₉ H ₂₄ O ₄	Cultured	[54]
3-Methylorsellinic acid (200)	182	C ₉ H ₁₀ O ₄	Cultured	[56]
O-Methyl-3-methylorsellinaldehyde dimer (201)	360	C ₂₀ H ₂₄ O ₆	Cultured	[56]
6-((S,3E,5E)-5,7-Dimethyl-2-oxonona-3,5-dien-1-yl)-2,4-dihydroxy-3-methylbenzaldehyde (202)	316	C ₁₉ H ₂₄ O ₄	Mutant strain cultured	[42]
Lecanoric acid (203)	318	C ₁₆ H ₁₄ O ₇	Deep-sea sediment, South China Sea	[31]
Myristic acid (204)	228	C ₁₄ H ₂₈ O ₂	<i>Turbinaria elatensis</i> (Brown alga, <i>Phaeophyceae</i>), Egyptian Red Sea, Ras Mohamed, South Sina, Egypt	[47]
Atrochrysone (205)	274	C ₁₅ H ₁₄ O ₅	Cultured	[56]
Asperoxide A (206)	234	C ₁₂ H ₂₆ O ₄	Deep-sea sediment, South China Sea	[31]

4. Bioactivities of *A. nidulans* Extracts

The extract of *E. nidulans* var. *acristata* displayed cytotoxic potential vs. different cell lines (mean IC₇₀ of 8.30 µg/mL) [43]. *A. nidulans* EtOAc extract culture broth had only moderate antibacterial effectiveness vs. *B. megaterium* [47]. It also (Conc. 30 µg/disc) exhibited selectivity vs. HEP-G2, compared with CCRF-CEM and CFU-GM, and potent inhibitory activity vs. HCV NS3/4A protease (IC₅₀ 30.0 µg/mL) [47]. *Rhizophora stylosa*-associated *A. nidulans* MA-143 exhibited antibacterial and brine shrimp lethality poten-

tial [34]. *E. nidulans* MFW39 mycelium extract (IC₅₀ 21.9 µg/mL) was found to have a more potent cytotoxic effect vs. the T47D cell line than broth extract (IC₅₀ 169.3 µg/mL) [36]. *Nyctanthes arbor-tristis*-associated *A. nidulans* extracts and fractions had moderate to potent growth inhibitory potential against NCI-H460, MCF-7, and HeLa cell lines in the SRB, where broth extract (LC₅₀ 95.0 and IC₅₀ 10.0 µg/mL) was most potent vs. HeLa, whereas mycelium petroleum ether insoluble fraction was most powerful vs. MCF-7 and NCI-H460 (IC₅₀ 18.0 and 10.0 µg/mL, respectively) [53].

5. Importance of *A. nidulans* and Its Enzymes

Enzymes have attracted growing interest because of their prevalent industrial applications in various fields, including pharmaceuticals, food, chemicals, and energy [81]. They can provide a cost-efficient and more efficacious process for industrial manufacturing, in comparison to chemical catalysts, since they are quite specific, eco-friendly, and function under mild conditions [82]. Therefore, there is a marked research direction towards producing enzymes with high yields to fulfill the increased industrial demand, as well as reducing the costs of enzyme production medium, isolation, and purification. In this regard, interest has been directed towards fungi as a prolific pool of enzymes.

In 2020, a review by Kumar summarized the published studies on the potential of *A. nidulans* as a producer of varied enzymes that have applications in diverse industrial processes [28]. Thus, in this work, the recent reports on *A. nidulans*'s enzymes are highlighted.

Two genes encoding β-isopropyl-malate dehydrogenase and six genes encoding BCAA (branched-chain amino acids; isoleucine, leucine, and valine) aminotransferase, which catalyze the leucine penultimate step and the BCAA final step biosynthesis, respectively, were identified utilizing *A. nidulans* genome sequence searches [83]. Fungal biosynthesis of BCAA is substantial enough for these fungi to cause disease in plants and human hosts. It is worth mentioning that humans lack the enzymes accountable for BCAA production; therefore, these enzymes could be a potential target of antifungal agents.

5.1. Aryl Alcohol Oxidase

AAO (Aryl alcohol oxidase) is an H₂O₂-providing extracellular enzyme that belongs to the glucose–ethanol–choline oxidoreductase. It converts aromatic alcohols to aldehydes and provides H₂O₂ for peroxidases to degrade lignin [84]; hence, it has a considerable function in lignin depolymerization, particularly in lignin polymer oxidation for the generation of fuels and chemicals [85].

A cost-effective medium for AAO high-yield production by recombinant *A. nidulans* was developed in a submerged culture that consisted of CSL (corn steep liquor), which is an inexpensive and rich source of nitrogen, vitamins, and minerals, in addition to NaNO₃ (13.8 g/L), CSL (26.4 g/L), and maltose (61.0 g/L). It was observed that the highest achieved AAO capacity was 1021 U/L, with a 0.75 g/L protein concentration [86].

5.2. Laccases

Laccases, belonging to the multi-copper oxidase family, accelerate the O₂ four-electron reduction to water with diverse non-phenolic and phenolic compound oxidation [16,87–89]. These features give them varied industrial applicability, including wine stabilization, denim-bleaching, detoxification and decolorization of dye-containing textiles and lignin-linked compound effluents, and pulp bio-bleaching for the paper industry [16,87–89].

From *A. nidulans* TTF-6, purified and crude laccases were employed to decolorize different dyes (e.g., methyl orange, Congo red, Victoria blue, methyl red, methyl violet, bromophenol blue, and Coomassie blue). At 40 °C, it was found that the crude enzyme needed a longer time treatment time (7 days) in comparison to the purified one (up to 48 h). Among the tested dyes, methyl red (azo dye) was taken away slowly relative to Victoria and Coomassie blue (blue-triphenylamines). A high decolorizing rate was noted at 40 °C compared to 20 °C [90].

5.3. Pectate Lyases and Nitroreductases

Pectin, a primary component of fibers, vegetables, cereals, and fruits, has a high molecular weight and is a complicated, acidic- and heterogeneous-structured polysaccharide that is hydrolyzed by pectinolytic enzymes. These enzymes have assorted industrial applicability in wine and fruit juice liquefaction, extraction, and clarification; in the fabric industry for separating plant fibers such as jute, flax, and hemp; in cotton fabric bio-preparation; in paper manufacture, treating paper and pulp mill effluents; and in amending black tea's quality [91]. These enzymes represent 25% of the global sales of food enzymes [92]. Among them, pectate lyases act on the pectate core internal α -1,4-linkage, having a crucial function in pectin breaking down.

In 2022, AnPL9 pectate lyase, a member of PL9 (polysaccharide-lyase family-9), was characterized and purified from *A. nidulans* that was expressed in *Pichia pastoris* [93]. It is the first stated fungi derived from the PL9 pectate lyase family. AnPL9 revealed high potential on GH (homogalacturonan), the pectin from apple and citrus peel. It converted tetra-galacturonic acid to digalact-uronic acid and 4,5-unsaturated digalacturonic acid. Additionally, AnPL9 possessed marked stability at 6–11 pH with a more than 4 polymerization degree of HG oligo-saccharides, indicating AnPL9 is beneficial for bio-technological usage in paper, food, and textile manufacturing [93].

Nitroreductases are implicated in nitro-heterocyclic and -aromatic compounds and quinone reduction. They have received marked attention for their usage in environmental pollutant biodegradation [94]. It was reported that *A. nidulans* produced nitroreductase boosted by menadione [95].

5.4. Xylanases

Xylanases are accountable for hydrolyzing xylan by cleaving the β -1,4 link, which is a main constituent of hemicellulose. They have remarkable applicability in various fields, such as food, paper and pulp, and bio-fuel industries, as well as in effluent and agro-waste treatment.

A study reported that optimized xylanase (1250 U/mL) production, with a productivity of 313 U/mL/day by recombinant *A. nidulans* in a 3 L stirred tank reactor, was a 400 rpm agitation rate and 2 vvm aeration rate utilizing batch fermentation. Further, the enzyme production elevated to 327 U/mL/day and 373 U/mL/day and maximum capacity increased to 1410 and 1572 U/mL, respectively, with repeated-batch and fed-batch fermentation, respectively [96].

5.5. Meta-Cresol Production

meta-Cresol is an industrially beneficial compound that is mainly generated by chemical means from fossil sources. It has been widely employed for farm chemicals, spices, dyes, and medicine production [97]. It is also a synthetic precursor for thymol, alpha-tocopherol, menthol, fenthion, sumithion, permethrin, diphenylamine, pressure-sensitive fuel, resin plasticizer, eikonogen, etc. Its mainstream production strategies involve extraction from coal tar and chemical means as cumene acidolysis and toluene-chlorination hydrolysis [98]. However, these strategies have apparent disadvantages: tiresome but unavoidable steps of m-cresol separation from the p-, m-, and o-cresol mixtures, environmental pollution, high costs, and less purity and titer [99].

The m-cresol overproduction utilizing modified *A. nidulans* FGSC no. A1145 Δ ST Δ EM was reported, which gave a gram-level titer utilizing starch (carbon source) [97]. Various strategies were carried out to increase m-cresol production, such as gene multiplication and promotor engineering, resulting in an increase to m-cresol production titers of 1.29 g/L and 2.03 g/L in shaking flasks and fed-batch culture, respectively. *A. nidulans* A1145 Δ ST Δ EM possessed better resistance to m-cresol than yeast, as it grew in the liquid medium, producing up to 2.5 g/L m-cresol. Thus, *A. nidulans* could be further engineered for m-cresol bio-production for industrial purposes [97].

5.6. Nanoparticles Synthesis

Metallic oxide NPs (nanoparticles) have extreme usage in supercapacitors, devices, batteries, and biosensors. Vijayanandan and Balakrishnan reported that *A. nidulans* is an efficient fungus for the synthesis of Co₃O₄ (cobalt oxide) NPs [100].

Additionally, the Co₃O₄ nanofluid synthesized employing *Nothapodytes foetida*-associated *A. nidulans* possessed good SAR (specific absorption rate), photothermal conversion efficiency, and a greater temperature gradient than water. The good solar energy absorption ability of this nanofluid indicates its convenience for direct-absorption solar thermal energy systems [101].

6. Conclusions

In the present work, 206 metabolites of varied classes, including different types of alkaloids, xanthines, quinones, depsidones, lactones, benzophenones, furanones, terpenoids, sterols, cerebrosides, fatty acids, polyketides, and others were characterized from *A. nidulans* and its teleomorph from 1953 to November 2022. The fungus has been collected from various sources, such as sea sediments, sponges, ascidians, algae, endophytes, soil, worms, and cultures.

Notably, a great number of metabolites were described in 2019 (39 compounds), 2013 (34 compounds), and 2016 (30 compounds).

Alkaloids of diverse types are the main metabolites reported from this fungus. They have been investigated for different biocapacities, such as antimicrobial, cytotoxic, anti-inflammation, antioxidant, antiviral, and Er α activities. Although there is a large number of reported metabolites, a limited number of them have been evaluated for their bioactivities.

Compounds **136** and **137** provide promising target molecules for further research as ER α (estrogen receptor α) inhibitors. Interestingly, **25** and **30** demonstrated marked tau aggregation inhibitory potential; therefore, they could be lead compounds for developing tau aggregation inhibitors in Alzheimer's disease and neurodegenerative tauopathies. Additionally, **36**, **56**, and **92** had potent antimicrobial potential as lead metabolites for antimicrobial agents. Moreover, **83**, **84**, **93**, **95**, and **104** revealed marked cytotoxic efficacies vs. different cell lines. Further in vivo and mechanistic investigations to elucidate and validate possible mechanisms for the active metabolites are needed, exploring the possible bioactivities of unevaluated metabolites using molecular dynamic and docking investigation.

It was found that metabolic-biosynthesis pathway engineering revealed the usefulness of creating profuse numbers of fascinating metabolites. Additionally, modifying the culture parameters and conditions affected metabolite production, such as ethanol stress. Several studies reported the usage of silent gene activation strategies, such as optimizing culture conditions (O₂ concentration, pH, and temperature), adding chemical elicitors (e.g., HDACi), and co-culturing with other microbes. These strategies could open a new direction for regulating the production of metabolites and play a pronounced role in elucidating cryptic natural metabolites that will assist in the future discovery of new metabolites. Further investigation of biosynthetic pathways of these metabolites is a prerequisite for allowing the reasonable engineering or refactoring of these pathways for industrial purposes. In addition, identifying genes accountable for these metabolites' formation could provide a chance for exploring the genetic potential of this fungus to discover novel metabolites. Therefore, using combined techniques such as genome mining, bio-informatics, fusion PCR, CRISPR (Clustered-Regularly-Interspaced Short-Palindromic Repeats), expression profiling, and culture manipulation has become progressively efficient in discovering and activating silent clusters in *A. nidulans* [102].

Author Contributions: Conceptualization, S.R.M.I. and G.A.M.; methodology, S.R.M.I., G.A.M. and S.G.A.M.; software, S.A.F. and K.F.G.; writing—original draft preparation, S.R.M.I., S.G.A.M. and G.A.M.; writing—review and editing, S.R.M.I., G.A.M., S.A.F. and K.F.G. resources, S.A.F. and K.F.G. All authors have read and agreed to the published version of the manuscript.

Funding: This research received no external funding.

Institutional Review Board Statement: Not applicable.

Informed Consent Statement: Not applicable.

Data Availability Statement: Not applicable.

Conflicts of Interest: The authors declare no conflict of interest.

Abbreviations

BEL-7402	Human hepatocellular carcinoma cell line
C28	Human colon Cell Line
CCRF-CEM	Human leukemia cell line
CCK-8	Cell counting kit-8
CD	Circular dichroism
ECD	Electronic circular dichroism
EtOH	Ethanol
EtOAc	Ethyl acetate
H-125	Human lung cancer cell line
HCT-116	Human colon cancer cell line
HepG2	Human hepatocellular liver carcinoma cell line
HeLa	Human cervical epitheloid carcinoma cell line
HL-60	Human promyelocytic leukemia cell line
HPLC	High-performance liquid chromatography
IC ₅₀	Half-maximal inhibitory concentration
K562	Human myelocytic leukemia cell line
KB	Human oral epidermoid carcinoma cell line
L1210	Mouse lymphocytic leukemia cell line
LD ₅₀	Half maximal lethal concentration
LPS	Lipopolysaccharide
MCF-7	Human breast adenocarcinoma cell line
MDA-MB-231	Human breast cancer cell line
MIC	Minimum inhibitory concentrations
MS	Mass spectrometry
MTT	3-(4,5-Dimethylthiazol-2-yl)-2,5-diphenyltetrazolium bromide
NCI-H460	Human lung cancer cell line
NMR	Nuclear magnetic resonance
NO	Nitric oxide
PC12	Rat brain cancer cell line
RP-18	Reversed phase-18
SRB	Sulforhodamine B
SiO ₂ CC	Silica gel column chromatography
T47D	Human breast cancer cell line
TLC	Thin layer chromatography
WiDr	Human colon adenocarcinoma cell line

References

1. Meyer, V.; Andersen, M.R.; Brakhage, A.A.; Braus, G.H.; Caddick, M.X.; Cairns, T.C.; de Vries, R.P.; Haarmann, T.; Hansen, K.; Hertz-Fowler, C. Current Challenges of Research on Filamentous Fungi in Relation to Human Welfare and a Sustainable Bio-Economy: A White Paper. *Fungal Biol. Biotechnol.* **2016**, *3*, 6. [\[CrossRef\]](#)
2. Meyer, V.; Basenko, E.Y.; Benz, J.P.; Braus, G.H.; Caddick, M.X.; Csukai, M.; De Vries, R.P.; Endy, D.; Frisvad, J.C.; Gunde-Cimerman, N. Growing a Circular Economy with Fungal Biotechnology: A White Paper. *Fungal Biol. Biotechnol.* **2020**, *7*, 5. [\[CrossRef\]](#)
3. Ibrahim, S.R.; Choudhry, H.; Asseri, A.H.; Elfaky, M.A.; Mohamed, S.G.; Mohamed, G.A. *Stachybotrys Chartarum*—A Hidden Treasure: Secondary Metabolites, Bioactivities, and Biotechnological Relevance. *J. Fungi* **2022**, *8*, 504. [\[CrossRef\]](#) [\[PubMed\]](#)
4. El-Agamy, D.S.; Ibrahim, S.R.; Ahmed, N.; Khoshhal, S.; Abo-Haded, H.M.; Elkablawy, M.A.; Aljuhani, N.; Mohamed, G.A. Aspernolide F, as a New Cardioprotective Butyrolactone Against Doxorubicin-Induced Cardiotoxicity. *Int. Immunopharmacol.* **2019**, *72*, 429–436. [\[CrossRef\]](#)

5. Ibrahim, S.R.; Elkhayat, E.S.; Mohamed, G.A.; Khedr, A.I.; Fouad, M.A.; Kotb, M.H.; Ross, S.A. Aspernolides F and G, New Butyrolactones from the Endophytic Fungus *Aspergillus terreus*. *Phytochem. Lett.* **2015**, *14*, 84–90. [\[CrossRef\]](#)
6. Chen, S.; Cai, R.; Liu, Z.; Cui, H.; She, Z. Secondary metabolites from mangrove-associated fungi: Source, chemistry and bioactivities. *Nat. Prod. Rep.* **2022**, *39*, 560–595. [\[CrossRef\]](#) [\[PubMed\]](#)
7. Ibrahim, S.R.; Mohamed, S.G.; Sindi, I.A.; Mohamed, G.A. Biologically Active Secondary Metabolites and Biotechnological Applications of Species of the Family Chaetomiaceae (Sordariales): An Updated Review from 2016 to 2021. *Mycol. Progress* **2021**, *20*, 595–639. [\[CrossRef\]](#)
8. Rustamova, N.; Bozorov, K.; Efferth, T.; Yili, A. Novel secondary metabolites from endophytic fungi: Synthesis and biological properties. *Phytochem. Rev.* **2020**, *19*, 425–448. [\[CrossRef\]](#)
9. Ibrahim, S.R.; Bagalagel, A.A.; Diri, R.M.; Noor, A.O.; Bakhsh, H.T.; Muhammad, Y.A.; Mohamed, G.A.; Omar, A.M. Exploring the Activity of Fungal Phenalenone Derivatives as Potential CK2 Inhibitors using Computational Methods. *J. Fungi* **2022**, *8*, 443. [\[CrossRef\]](#)
10. Ibrahim, S.R.; Sirwi, A.; Eid, B.G.; Mohamed, S.G.; Mohamed, G.A. Fungal depsides—Naturally Inspiring Molecules: Biosynthesis, Structural Characterization, and Biological Activities. *Metabolites* **2021**, *11*, 683. [\[CrossRef\]](#)
11. Ibrahim, S.R.M.; Fadil, S.A.; Fadil, H.A.; Eshmawi, B.A.; Mohamed, S.G.A.; Mohamed, G.A. Fungal Naphthalenones; Promising Metabolites for Drug Discovery: Structures, Biosynthesis, Sources, and Pharmacological Potential. *Toxins* **2022**, *14*, 154. [\[CrossRef\]](#) [\[PubMed\]](#)
12. Ibrahim, S.R.M.; Mohamed, G.A.; Al Haidari, R.A.; Zayed, M.F.; El-Kholy, A.A.; Elkhayat, E.S.; Ross, S.A. Fusarithioamide B, a New Benzamide Derivative from the Endophytic Fungus *Fusarium Chlamydosporium* with Potent Cytotoxic and Antimicrobial Activities. *Bioorg. Med. Chem.* **2018**, *26*, 786–790. [\[CrossRef\]](#)
13. Ibrahim, S.R.; Abdallah, H.M.; Elkhayat, E.S.; Al Musayeib, N.M.; Asfour, H.Z.; Zayed, M.F.; Mohamed, G.A. Fusaripeptide A: New Antifungal and Anti-Malarial Cyclodepsipeptide from the Endophytic Fungus *Fusarium* sp. *J. Asian Nat. Prod. Res.* **2018**, *20*, 75–85. [\[CrossRef\]](#) [\[PubMed\]](#)
14. Ortega, H.E.; Torres-Mendoza, D.; Caballero E., Z.; Cubilla-Rios, L. Structurally uncommon secondary metabolites derived from endophytic fungi. *J. Fungi* **2021**, *7*, 570. [\[CrossRef\]](#) [\[PubMed\]](#)
15. Ibrahim, S.R.M.; Sirwi, A.; Eid, B.G.; Mohamed, S.G.A.; Mohamed, G.A. Bright Side of *Fusarium Oxysporum*: Secondary Metabolites Bioactivities and Industrial Relevance in Biotechnology and Nanotechnology. *J. Fungi* **2021**, *7*, 943. [\[CrossRef\]](#)
16. Hareeri, R.H.; Aldurdunji, M.M.; Abdallah, H.M.; Alqarni, A.A.; Mohamed, S.G.A.; Mohamed, G.A.; Ibrahim, S.R.M. *Aspergillus Ochraceus*: Metabolites, Bioactivities, Biosynthesis, and Biotechnological Potential. *Molecules* **2022**, *27*, 6759. [\[CrossRef\]](#)
17. Klich, M.A. Health Effects of *Aspergillus* in Food and Air. *Toxicol. Ind. Health* **2009**, *25*, 657–667. [\[CrossRef\]](#)
18. Bennett Scott, E.; Bakerand Joan, W. An Overview of the Genus *Aspergillus*. In *The Aspergilli*; CRC Press: Boca Raton, FL, USA, 2007; pp. 23–34.
19. Frisvad, J.C.; Møller, L.L.H.; Larsen, T.O.; Kumar, R.; Arnau, J. Safety of the Fungal Workhorses of Industrial Biotechnology: Update on the Mycotoxin and Secondary Metabolite Potential of *Aspergillus Niger*, *Aspergillus Oryzae*, and *Trichoderma Reesei*. *Appl. Microbiol. Biotechnol.* **2018**, *102*, 9481–9515. [\[CrossRef\]](#) [\[PubMed\]](#)
20. Ibrahim, S.R.; Mohamed, G.A.; Khedr, A.I. Γ -Butyrolactones from *Aspergillus* Species: Structures, Biosynthesis, and Biological Activities. *Nat. Prod. Commun.* **2017**, *12*, 791–800. [\[CrossRef\]](#)
21. Zhang, X.; Li, Z.; Gao, J. Chemistry and Biology of Secondary Metabolites from *Aspergillus* Genus. *Nat. Prod. J.* **2018**, *8*, 275–304. [\[CrossRef\]](#)
22. Abdel-Azeem, A.M.; Abdel-Azeem, M.A.; Abdul-Hadi, S.Y.; Darwish, A.G. *Aspergillus*: Biodiversity, ecological significances, and industrial applications. In *Recent Advancement in White Biotechnology through Fungi*; Springer: Berlin/Heidelberg, Germany, 2019; pp. 121–179.
23. Romero, S.M.; Giudicessi, S.L.; Vitale, R.G. Is the Fungus *Aspergillus* a Threat to Cultural Heritage? *J. Cult. Herit.* **2021**, *51*, 107–124. [\[CrossRef\]](#)
24. Ahluwalia, S.K.; Matsui, E.C. Indoor Environmental Interventions for Furry Pet Allergens, Pest Allergens, and Mold: Looking to the Future. *J. Allergy Clin. Immunol. Pract.* **2018**, *6*, 9–19. [\[CrossRef\]](#)
25. Segal, B.H.; DeCarlo, E.S.; Kwon-Chung, K.J.; Malech, H.L.; Gallin, J.I.; Holland, S.M. *Aspergillus Nidulans* Infection in Chronic Granulomatous Disease. *Medicine* **1998**, *77*, 345–354. [\[CrossRef\]](#)
26. Henriët, S.S.; Verweij, P.E.; Warris, A. *Aspergillus Nidulans* and Chronic Granulomatous Disease: A Unique Host–pathogen Interaction. *J. Infect. Dis.* **2012**, *206*, 1128–1137. [\[CrossRef\]](#) [\[PubMed\]](#)
27. Tavakoli, M.; Hedayati, M.T.; Mirhendi, H.; Nouripour-Sisakht, S.; Hedayati, N.; Saghafi, F.; Mamishi, S. The First Rare and Fatal Case of Invasive Aspergillosis of Spinal Cord due to *Aspergillus Nidulans* in an Iranian Child with Chronic Granulomatosis Disease: Review of Literature. *Curr. Med. Mycol.* **2020**, *6*, 55. [\[CrossRef\]](#)
28. Kumar, A. *Aspergillus nidulans*: A Potential Resource of the Production of the Native and Heterologous Enzymes for Industrial Applications. *Int. J. Microbiol.* **2020**, *2020*, 8894215. [\[CrossRef\]](#)
29. Brandl, J.; Andersen, M.R. *Aspergilli*: Models for Systems Biology in Filamentous Fungi. *Curr. Opin. Syst. Biol.* **2017**, *6*, 67–73. [\[CrossRef\]](#)
30. Yang, S.; Li, X.; Xu, G.; Li, X.; An, C.; Wang, B. Antibacterial Anthraquinone Derivatives Isolated from a Mangrove-Derived Endophytic Fungus *Aspergillus nidulans* by Ethanol Stress Strategy. *J. Antibiot.* **2018**, *71*, 778–784. [\[CrossRef\]](#)

31. Lü, F.; Li, X.; Chi, L.; Meng, L.; Wang, B. A New Acyclic Peroxide from *Aspergillus nidulans* SD-531, a Fungus obtained from Deep-Sea Sediment of Cold Spring in the South China Sea. *J. Oceanol. Limnol.* **2020**, *38*, 1225–1232. [\[CrossRef\]](#)
32. Ninomiya, A.; Urayama, S.; Hagiwara, D. Antibacterial Diphenyl Ether Production Induced by Co-Culture of *Aspergillus nidulans* and *Aspergillus fumigatus*. *Appl. Microbiol. Biotechnol.* **2022**, *106*, 4169–4185. [\[CrossRef\]](#) [\[PubMed\]](#)
33. Li, Q.; Chen, C.; He, Y.; Wei, M.; Cheng, L.; Kang, X.; Wang, J.; Hao, X.; Zhu, H.; Zhang, Y. Prenylated Quinolinone Alkaloids and Prenylated Isoindolinone Alkaloids from the Fungus *Aspergillus nidulans*. *Phytochemistry* **2020**, *169*, 112177. [\[CrossRef\]](#) [\[PubMed\]](#)
34. An, C.; Li, X.; Luo, H.; Li, C.; Wang, M.; Xu, G.; Wang, B. 4-Phenyl-3, 4-Dihydroquinolone Derivatives from *Aspergillus nidulans* MA-143, an Endophytic Fungus Isolated from the Mangrove Plant *Rhizophora stylosa*. *J. Nat. Prod.* **2013**, *76*, 1896–1901. [\[CrossRef\]](#)
35. An, C.; Li, X.; Li, C.; Wang, M.; Xu, G.; Wang, B. Aniquinazolines A–D, Four New Quinazolinone Alkaloids from Marine-Derived Endophytic Fungus *Aspergillus nidulans*. *Mar. Drugs* **2013**, *11*, 2682–2694. [\[CrossRef\]](#) [\[PubMed\]](#)
36. Nursid, M.; Ekowati, C.; Murwantoko; Wahyuono, S. Isolation and Identification of Emestrin from *Emericella nidulans* and Investigation of its Anticancer Properties. *Microbiol. Indones.* **2011**, *5*, 3. [\[CrossRef\]](#)
37. Nursid, M.; Namirah, I.; Cahyana, A.H.; Fajarningsih, N.D.; Chasanah, E. Emestrin B: Epipolythiodioxypiperazine from Marine Derived Fungus *Emericella nidulans*. *J. Med. Bioeng.* **2015**, *4*, 441–445. [\[CrossRef\]](#)
38. Zhang, P.; Li, X.; Li, X.; Wang, B. New Indole-Diterpenoids from the Algal-Associated Fungus *Aspergillus nidulans*. *Phytochem. Lett.* **2015**, *12*, 182–185. [\[CrossRef\]](#)
39. Zhou, H.; Sun, X.; Li, N.; Che, Q.; Zhu, T.; Gu, Q.; Li, D. Isoindolone-Containing Meroperpenoids from the Endophytic Fungus *Emericella nidulans* HDN12–249. *Org. Lett.* **2016**, *18*, 4670–4673. [\[CrossRef\]](#)
40. Li, Q.; Chen, C.; Wei, M.; Dai, C.; Cheng, L.; Tao, J.; Li, X.; Wang, J.; Sun, W.; Zhu, H. Niduterpenoids A and B: Two Sesterterpenoids with a Highly Congested Hexacyclic 5/5/5/5/3/5 Ring System from the Fungus *Aspergillus nidulans*. *Org. Lett.* **2019**, *21*, 2290–2293. [\[CrossRef\]](#)
41. Li, Q.; Zheng, Y.; Fu, A.; Wei, M.; Kang, X.; Chen, C.; Zhu, H.; Zhang, Y. 30-Norlanostane Triterpenoids and Steroid Derivatives from the Endophytic Fungus *Aspergillus nidulans*. *Phytochemistry* **2022**, *201*, 113257. [\[CrossRef\]](#)
42. Somoza, A.D.; Lee, K.; Chiang, Y.; Oakley, B.R.; Wang, C.C. Reengineering an Azaphilone Biosynthesis Pathway in *Aspergillus nidulans* to Create Lipxygenase Inhibitors. *Org. Lett.* **2012**, *14*, 972–975. [\[CrossRef\]](#)
43. Sanchez, J.F.; Entwistle, R.; Hung, J.; Yaegashi, J.; Jain, S.; Chiang, Y.; Wang, C.C.; Oakley, B.R. Genome-Based Deletion Analysis Reveals the Prenyl Xanthone Biosynthesis Pathway in *Aspergillus nidulans*. *J. Am. Chem. Soc.* **2011**, *133*, 4010–4017. [\[CrossRef\]](#)
44. Pockrandt, D.; Ludwig, L.; Fan, A.; König, G.M.; Li, S. New Insights into the Biosynthesis of Prenylated Xanthones: Xptb from *Aspergillus nidulans* Catalyses an O-Prenylation of Xanthones. *Chembiochem* **2012**, *13*, 2764–2771. [\[CrossRef\]](#) [\[PubMed\]](#)
45. Kralj, A.; Kehraus, S.; Krick, A.; Eguereva, E.; Kelter, G.; Maurer, M.; Wortmann, A.; Fiebig, H.; König, G.M. Arugosins G and H: Prenylated Polyketides from the Marine-Derived Fungus *Emericella nidulans* Var. a Cristata. *J. Nat. Prod.* **2006**, *69*, 995–1000. [\[CrossRef\]](#) [\[PubMed\]](#)
46. Kawahara, N.; Sekita, S.; Satake, M.; Udagawa, S.; Kawai, K. Structures of a New Dihydroxanthone Derivative, Nidulalin A, and a New Benzophenone Derivative, Nidulalin B, from *Emericella nidulans*. *Chem. Pharm. Bull.* **1994**, *42*, 1720–1723. [\[CrossRef\]](#)
47. Hawas, U.W.; El-Kassem, L.T.; Ahmed, E.F.; Emam, M. In-Vitro Bioassays on the Metabolites of the Fungus *Emericella nidulans* Isolated from the Egyptian Red Sea Algae. *Egypt. Pharm. J.* **2012**, *11*, 124.
48. Ishida, M.; Hamasaki, T.; Hatsuda, Y. The Structure of Two New Metabolites, Emerin and Emericellin, from *Aspergillus nidulans*. *Agric. Biol. Chem.* **1975**, *39*, 2181–2184. [\[CrossRef\]](#)
49. Yaegashi, J.; Praseuth, M.B.; Tyan, S.; Sanchez, J.F.; Entwistle, R.; Chiang, Y.; Oakley, B.R.; Wang, C.C. Molecular Genetic Characterization of the Biosynthesis Cluster of a Prenylated Isoindolinone Alkaloid Aspermidine A in *Aspergillus nidulans*. *Org. Lett.* **2013**, *15*, 2862–2865. [\[CrossRef\]](#)
50. Nasr, H.M.; Hawas, U.W.; Mousa, S.A.; Alasmaey, M.; Ahmed, E.F. Isolation and Identification of *Emericella nidulans* Secondary Metabolites. *Chem. Res. J.* **2018**, *3*, 114–119.
51. Aukamp, P.J.; Holzapfel, C.W. Polyhydroxyanthraquinones from *Aspergillus Versicolor*, *Aspergillus nidulans* and *Bipolaris* Sp. their Significance in Relation to Biogenetic Theories on Aflatoxin B1. *S. Afr. J. Chem.* **1970**, *23*, 40–56.
52. Furukawa, T.; Fukuda, T.; Nagai, K.; Uchida, R.; Tomoda, H. Helvafuranone Produced by the Fungus *Aspergillus nidulans* BF0142 Isolated from Hot Spring-Derived Soil. *Nat. Prod. Commun.* **2016**, *11*, 1001–1003. [\[CrossRef\]](#)
53. Sana, T.; Siddiqui, B.S.; Shahzad, S.; Farooq, A.D.; Siddiqui, F.; Sattar, S.; Begum, S. Antiproliferative Activity and Characterization of Metabolites of *Aspergillus nidulans*: An Endophytic Fungus from *Nyctanthes Arbor-Tristis* Linn. Against Three Human Cancer Cell Lines. *Med. Chem.* **2019**, *15*, 352–359. [\[CrossRef\]](#)
54. Paranjape, S.R.; Chiang, Y.; Sanchez, J.F.; Entwistle, R.; Wang, C.C.; Oakley, B.R.; Gamblin, T.C. Inhibition of Tau Aggregation by Three *Aspergillus nidulans* Secondary Metabolites: 2, Ω -Dihydroxyemodin, Asperthecin, and Asperbenzaldehyde. *Planta Med.* **2014**, *80*, 77–85. [\[CrossRef\]](#)
55. Brown, D.W.; Salvo, J.J. Isolation and Characterization of Sexual Spore Pigments from *Aspergillus nidulans*. *Appl. Environ. Microbiol.* **1994**, *60*, 979–983. [\[CrossRef\]](#) [\[PubMed\]](#)
56. Grau, M.F.; Entwistle, R.; Oakley, C.E.; Wang, C.C.; Oakley, B.R. Overexpression of an LaeA-Like Methyltransferase Upregulates Secondary Metabolite Production in *Aspergillus nidulans*. *ACS Chem. Biol.* **2019**, *14*, 1643–1651. [\[CrossRef\]](#)
57. Lin, H.; Lyu, H.; Zhou, S.; Yu, J.; Keller, N.P.; Chen, L.; Yin, W. Deletion of a Global Regulator LaeB Leads to the Discovery of Novel Polyketides in *Aspergillus nidulans*. *Org. Biomol. Chem.* **2018**, *16*, 4973–4976. [\[CrossRef\]](#)

58. Xing, C.; Wu, J.; Xia, J.; Fan, S.; Yang, X. Steroids and Anthraquinones from the Deep-Sea-Derived Fungus *Aspergillus nidulans* MCCC 3A00050. *Biochem. Syst. Ecol.* **2019**, *83*, 103–105. [\[CrossRef\]](#)
59. Ibrahim, S.R.M.; Mohamed, G.A.; Al Haidari, R.A.; El-Kholy, A.A.; Zayed, M.F.; Khayat, M.T. Biologically Active Fungal Depsidones: Chemistry, Biosynthesis, Structural Characterization, and Bioactivities. *Fitoterapia* **2018**, *129*, 317–365. [\[CrossRef\]](#) [\[PubMed\]](#)
60. Dean, F.M.; Robertson, A.; ROBERTS, J.C.; Raper, K.B. Nidulin and 'Ustin': Two Chlorine-Containing Metabolic Products of *Aspergillus nidulans*. *Nature* **1953**, *172*, 344. [\[CrossRef\]](#) [\[PubMed\]](#)
61. Sierankiewicz, J.; Gatenbeck, S. A New Depsidone from *Aspergillus nidulans*. *Acta Chem. Scand.* **1972**, *26*, 455–458. [\[CrossRef\]](#)
62. Scherlach, K.; Hertweck, C. Discovery of Aspoquinolones A–D, Prenylated Quinoline-2-One Alkaloids from *Aspergillus nidulans*, Motivated by Genome Mining. *Org. Biomol. Chem.* **2006**, *4*, 3517–3520. [\[CrossRef\]](#)
63. Perry, M.J.; Makins, J.F.; Adlard, M.W.; Holt, G. Aspergillilic Acids Produced by Mixed Cultures of *Aspergillus Flavus* and *Aspergillus nidulans*. *J. Gen. Microbiol.* **1984**, *130*, 319–323. [\[CrossRef\]](#)
64. Ryan, K.L.; Akhmedov, N.G.; Panaccione, D.G. Identification and Structural Elucidation of Ergotryptamine, a New Ergot Alkaloid Produced by Genetically Modified *Aspergillus nidulans* and Natural Isolates of *Epichloë* Species. *J. Agric. Food Chem.* **2015**, *63*, 61–67. [\[CrossRef\]](#)
65. Scherlach, K.; Schuemann, J.; Dahse, H.; Hertweck, C. Aspernidine A and B, Prenylated Isoindolinone Alkaloids from the Model Fungus *Aspergillus nidulans*. *J. Antibiot.* **2010**, *63*, 375–377. [\[CrossRef\]](#)
66. McCorkindale, N.J.; Hayes, D.; Johnston, G.A.; Clutterbuck, A.J. N-Acetyl-6-Hydroxytryptophan a Natural Substrate of a Monophenol Oxidase from *Aspergillus nidulans*. *Phytochemistry* **1983**, *22*, 1026–1028. [\[CrossRef\]](#)
67. Kaczka, E.A.; Dulaney, E.L.; Gitterman, C.O.; Woodruff, H.B.; Folkers, K. Isolation and Inhibitory Effects on KB Cell Cultures of 3'-Deoxyadenosine from *Aspergillus nidulans* (Eidam) Wint. *Biochem. Biophys. Res. Commun.* **1964**, *14*, 452–455. [\[CrossRef\]](#) [\[PubMed\]](#)
68. Tarawneh, A.H.; León, F.; Radwan, M.M.; Rosa, L.H.; Cutler, S.J. Secondary Metabolites from the Fungus *Emericella nidulans*. *Nat. Prod. Commun.* **2013**, *8*, 1285–1288. [\[CrossRef\]](#)
69. Henke, M.T.; Soukup, A.A.; Goering, A.W.; McClure, R.A.; Thomson, R.J.; Keller, N.P.; Kelleher, N.L. New Aspercryptins, Lipopeptide Natural Products, Revealed by HDAC Inhibition in *Aspergillus nidulans*. *ACS Chem. Biol.* **2016**, *11*, 2117–2123. [\[CrossRef\]](#) [\[PubMed\]](#)
70. Benz, F.; Knüsel, F.; Nüesch, J.; Treichler, H.; Voser, W.; Nyfeler, R.; Keller-Schierlein, W. Stoffwechselprodukte Von Mikroorganismen 143. Mitteilung. Echinocandin B, Ein Neuartiges Polypeptid-antibioticum Aus *Aspergillus nidulans* Var. Echinulatus: Isolierung Und Bausteine. *Helv. Chim. Acta* **1974**, *57*, 2459–2477. [\[CrossRef\]](#) [\[PubMed\]](#)
71. Bromann, K.; Viljanen, K.; Moreira, V.M.; Yli-Kauhala, J.; Ruohonen, L.; Nakari-Setälä, T. Isolation and Purification of Ent-Pimara-8 (14), 15-Diene from Engineered *Aspergillus nidulans* by Accelerated Solvent Extraction Combined with HPLC. *Anal. Methods* **2014**, *6*, 1227–1234. [\[CrossRef\]](#)
72. Rodríguez-Urra, A.B.; Jiménez, C.; Nieto, M.I.; Rodríguez, J.; Hayashi, H.; Ugalde, U. Signaling the Induction of Sporulation Involves the Interaction of Two Secondary Metabolites in *Aspergillus nidulans*. *ACS Chem. Biol.* **2012**, *7*, 599–606. [\[CrossRef\]](#)
73. Gealt, M.A. Isolation of B-Amyrin from the Fungus *Aspergillus nidulans*. *J. Gen. Microbiol.* **1983**, *129*, 543–546. [\[CrossRef\]](#)
74. Shapiro, B.E.; Gealt, M.A. Ergosterol and Lanosterol from *Aspergillus nidulans*. *J. Gen. Microbiol.* **1982**, *128*, 1053–1056. [\[CrossRef\]](#) [\[PubMed\]](#)
75. Hamasaki, T.; Nakajima, H.; Yokota, T.; Kimura, Y. A New Metabolite, 3-Carboxy-2, 4-Diphenyl-but-2-Enoic Anhydride, Produced by *Aspergillus nidulans*. *Agric. Biol. Chem.* **1983**, *47*, 891–892. [\[CrossRef\]](#)
76. Chiang, Y.; Oakley, C.E.; Ahuja, M.; Entwistle, R.; Schultz, A.; Chang, S.; Sung, C.T.; Wang, C.C.; Oakley, B.R. An Efficient System for Heterologous Expression of Secondary Metabolite Genes in *Aspergillus nidulans*. *J. Am. Chem. Soc.* **2013**, *135*, 7720–7731. [\[CrossRef\]](#)
77. Fukuyama, K.; Katsube, Y.; Noda, A.; Hamasaki, T.; Hatsuda, Y. Absolute Configurations of Asperlin, a Metabolite of *Aspergillus nidulans*, and its Related Compounds. *Bull. Chem. Soc. Jpn.* **1978**, *51*, 3175–3181. [\[CrossRef\]](#)
78. Argoudelis, A.D.; Zieserl, J.F. The Structure of U-13,933, a New Antibiotic. *Tetrahedron Lett.* **1966**, *7*, 1969–1973. [\[CrossRef\]](#)
79. Mazur, P.; Meyers, H.V.; Nakanishi, K.; Champe, S.P. Structural Elucidation of Sporogenic Fatty Acid Metabolites from *Aspergillus nidulans*. *Tetrahedron Lett.* **1990**, *31*, 3837–3840. [\[CrossRef\]](#)
80. Li, Q.; Chen, C.; He, Y.; Guan, D.; Cheng, L.; Hao, X.; Wei, M.; Zheng, Y.; Liu, C.; Li, X. Emeriones A–C: Three Highly Methylated Polyketides with Bicyclo [4.2. 0] Octene and 3, 6-Dioxabicyclo [3.1. 0] Hexane Functionalities from *Emericella nidulans*. *Org. Lett.* **2019**, *21*, 5091–5095. [\[CrossRef\]](#)
81. Singh, R.; Kumar, M.; Mittal, A.; Mehta, P.K. Microbial Enzymes: Industrial Progress in 21st Century. *3 Biotech.* **2016**, *6*, 174. [\[CrossRef\]](#) [\[PubMed\]](#)
82. Choi, J.; Han, S.; Kim, H. Industrial Applications of Enzyme Biocatalysis: Current Status and Future Aspects. *Biotechnol. Adv.* **2015**, *33*, 1443–1454. [\[CrossRef\]](#) [\[PubMed\]](#)
83. Steyer, J.T.; Downes, D.J.; Hunter, C.C.; Migeon, P.A.; Todd, R.B. Duplication and Functional Divergence of Branched-Chain Amino Acid Biosynthesis Genes in *Aspergillus nidulans*. *Mbio* **2021**, *12*, 768. [\[CrossRef\]](#)
84. Hernández-Ortega, A.; Ferreira, P.; Martínez, A.T. Fungal Aryl-Alcohol Oxidase: A Peroxide-Producing Flavoenzyme Involved in Lignin Degradation. *Appl. Microbiol. Biotechnol.* **2012**, *93*, 1395–1410. [\[CrossRef\]](#)

85. Mathieu, Y.; Piumi, F.; Valli, R.; Aramburu, J.C.; Ferreira, P.; Faulds, C.B.; Record, E. Activities of Secreted Aryl Alcohol Quinone Oxidoreductases from *Pycnoporus Cinnabarinus* Provide Insights into Fungal Degradation of Plant Biomass. *Appl. Environ. Microbiol.* **2016**, *82*, 2411–2423. [\[CrossRef\]](#)
86. Liu, E.; Li, M.; Abdella, A.; Wilkins, M.R. Development of a Cost-Effective Medium for Submerged Production of Fungal Aryl Alcohol Oxidase using a Genetically Modified *Aspergillus nidulans* Strain. *Bioresour. Technol.* **2020**, *305*, 123038. [\[CrossRef\]](#)
87. Ibrahim, S.R.; Altyar, A.E.; Mohamed, S.G.; Mohamed, G.A. Genus *Thielavia*: Phytochemicals, Industrial Importance and Biological Relevance. *Nat. Prod. Res.* **2021**, *36*, 5108–5123. [\[CrossRef\]](#)
88. Mohamed, G.A.; Ibrahim, S.R. Untapped Potential of Marine-Associated *Cladosporium* Species: An Overview on Secondary Metabolites, Biotechnological Relevance, and Biological Activities. *Mar. Drugs* **2021**, *19*, 645. [\[CrossRef\]](#)
89. Ibrahim, S.R.M.; Mohamed, S.G.A.; Altyar, A.E.; Mohamed, G.A. Natural Products of the Fungal Genus *Humicola*: Diversity, Biological Activity, and Industrial Importance. *Curr. Microbiol.* **2021**, *78*, 2488–2509. [\[CrossRef\]](#)
90. Sahay, S.; Chaurse, V.; Chauhan, D. Laccase from *Aspergillus nidulans* TTF6 Showing Pb Activation for Smaller Substrates and Dyes Remediation in all Climates. In *Proceedings of the National Academy of Sciences, India Section B: Biological Sciences*; Springer: Berlin/Heidelberg, Germany, 2020; Volume 90, pp. 143–150.
91. Dutta, N.; Mukhopadhyay, A.; Dasgupta, A.K.; Chakrabarti, K. Nanotechnology Enabled Enhancement of Enzyme Activity and Thermostability: Study on Impaired Pectate Lyase from Attenuated *Macrophomina Phaseolina* in Presence of Hydroxyapatite Nanoparticle. *PLoS ONE* **2013**, *8*, e63567. [\[CrossRef\]](#)
92. Oumer, O.J. Pectinase: Substrate, Production and their Biotechnological Applications. *Int. J. Environ. Agric. Biotechnol.* **2017**, *2*, 238761. [\[CrossRef\]](#)
93. Suzuki, H.; Morishima, T.; Handa, A.; Tsukagoshi, H.; Kato, M.; Shimizu, M. Biochemical Characterization of a Pectate Lyase AnPL9 from *Aspergillus nidulans*. *Appl. Biochem. Biotechnol.* **2022**, *194*, 5627–5643. [\[CrossRef\]](#)
94. Roldán, M.D.; Pérez-Reinado, E.; Castillo, F.; Moreno-Vivián, C. Reduction of Polynitroaromatic Compounds: The Bacterial Nitroreductases. *FEMS Microbiol. Rev.* **2008**, *32*, 474–500. [\[CrossRef\]](#)
95. Zhou, Y.; Lv, H.; Li, H.; Li, J.; Yan, Y.; Liu, F.; Hao, W.; Zhou, Z.; Wang, P.; Zhou, S. Nitroreductase Increases Menadione-Mediated Oxidative Stress in *Aspergillus nidulans*. *Appl. Environ. Microbiol.* **2021**, *87*, 1758. [\[CrossRef\]](#)
96. Abdella, A.; Segato, F.; Wilkins, M.R. Optimization of Process Parameters and Fermentation Strategy for Xylanase Production in a Stirred Tank Reactor using a Mutant *Aspergillus nidulans* Strain. *Biotechnol. Rep.* **2020**, *26*, e00457. [\[CrossRef\]](#)
97. Wang, W.; An, C.; Yao, Y.; Meng, X.; Gao, S. De Novo Biosynthesis and Gram-Level Production of M-Cresol in *Aspergillus nidulans*. *Appl. Microbiol. Biotechnol.* **2021**, *105*, 6333–6343. [\[CrossRef\]](#)
98. Bing, X.; Wang, Z.; Wei, F.; Gao, J.; Xu, D.; Zhang, L.; Wang, Y. Separation of M-Cresol from Coal Tar Model Oil using Propylamine-Based Ionic Liquids: Extraction and Interaction Mechanism Exploration. *ACS Omega* **2020**, *5*, 23090–23098. [\[CrossRef\]](#)
99. Vrsaljko, D.; Haramija, V.; Hadži-Skerlev, A. Determination of Phenol, M-Cresol and O-Cresol in Transformer Oil by HPLC Method. *Electr. Power Syst. Res.* **2012**, *93*, 24–31. [\[CrossRef\]](#)
100. Vijayanandan, A.S.; Balakrishnan, R.M. Biosynthesis of Cobalt Oxide Nanoparticles using Endophytic Fungus *Aspergillus nidulans*. *J. Environ. Manag.* **2018**, *218*, 442–450. [\[CrossRef\]](#)
101. Vijayanandan, A.S.; Valappil, R.S.K.; Balakrishnan, R.M. Evaluation of Photothermal Properties for Absorption of Solar Energy by Co3O4 Nanofluids Synthesized using Endophytic Fungus *Aspergillus nidulans*. *Sustain. Energy Technol. Assess.* **2020**, *37*, 100598. [\[CrossRef\]](#)
102. Caesar, L.K.; Kelleher, N.L.; Keller, N.P. In the Fungus Where it Happens: History and Future Propelling *Aspergillus nidulans* as the Archetype of Natural Products Research. *Fungal Genet. Biol.* **2020**, *144*, 103477. [\[CrossRef\]](#)

Disclaimer/Publisher's Note: The statements, opinions and data contained in all publications are solely those of the individual author(s) and contributor(s) and not of MDPI and/or the editor(s). MDPI and/or the editor(s) disclaim responsibility for any injury to people or property resulting from any ideas, methods, instructions or products referred to in the content.